Scientific Research Publishing

Computational Molecular Bioscience, 2022, 12, 20-57
https://www.scirp.org/journal/cmb
ISSN Online: 2165-3453
ISSN Print: 2165-3445

Analysis of Proteotranscriptomics Landscape Reveals Differentially Regulated Pathways in *Toxoplasma gondii* Infected Mouse Liver

Tanzina Tarannum[1], Md. Saruar Alam[2], Atiqur Rahman[1], Sajib Chakraborty[2], Hossain Uddin Shekhar[2], Taibur Rahman[1]*

[1]Laboratory of Infection Biology, Department of Biochemistry and Molecular Biology, University of Dhaka, Dhaka, Bangladesh
[2]Laboratory Clinical Biochemistry and Translational Medicine, Department of Biochemistry and Molecular Biology, University of Dhaka, Dhaka, Bangladesh
Email: *taibur@du.ac.bd

How to cite this paper: Tarannum, T., Alam, M.S., Rahman, A., Chakraborty, S., Shekhar, H.U. and Rahman, T. (2022) Analysis of Proteotranscriptomics Landscape Reveals Differentially Regulated Pathways in *Toxoplasma gondii* Infected Mouse Liver. *Computational Molecular Bioscience*, **12**, 20-57.
https://doi.org/10.4236/cmb.2022.121003

Received: January 3, 2022
Accepted: February 27, 2022
Published: March 10, 2022

Abstract

Toxoplasma gondii (*T. gondii*) an intracellular protozoan parasite, infects mammals including human population world-wide. Upon primary infection, the parasite contributes to mild flu like symptoms in immune competent host, but life threatening complication is seen in immune compromised patients and in pregnant women. Understanding the host-parasite interaction is critical for understanding the pathogenesis and biology parasite reactivation in the host. In this study, we used proteotrasncriptomics analyses by integrating the transcriptomics and proteomics data of *T. gondii* infected mouse liver to uncover the effector molecules responsible for disease pathogenesis that can be used as candidate markers for diagnosis and drug target. With this aim, we systematically integrated transcriptomicand proteomic data, representing the parasite infected mouse liver. Out of 2758 differentially expressed genes (DEGs) and 301 differentially expressed proteins (DEPs), 159 overlapping genes were identified. Among them, 86 genes were upregulated and 72 were downregulated in their respective mRNA and protein levels in the infected condition. Gene Ontology (GO) analysis revealed that the upregulated genes were mostly associated with immune system processes whereas the downregulated genes were involved in oxidation-reduction process and metabolism of lipid, and fatty acids. Protein-protein interaction (PPI) network analysis uncovered an interaction-hub including, Psmb8, Psmb9 and Tap1 for upregulated proteins and Cyp1A2, Cyp4A10 and Cyp3A11 for down-regulated proteins. Further studies are needed to validating these effector molecules. These molecules are likely to play a vital role in disease pathogenesis, as well as can be used as potential diagnostic marker and drug target candidates.

Keywords

Toxoplasma gondii, Transcriptome, Proteome, Mouse Liver, Differentially Expressed Genes and Proteins, Gene Ontology Analysis, Protein-Protein Interaction, Hub-Proteins, Homology Modeling, Effector Molecules

1. Introduction

Toxoplasmosis is one of the major public health problems world-wide, and is caused by an apicomplexian protozoan parasite *Toxoplasma gondii* [1]. *T. gondii is* unique in nature, because it can infect all type of nucleated cells of warm-blooded animals and humans [2]. Major transmission routes of the parasite can be oocysts contaminated foods, water and vegetables [3], ingestion of under-cooked meat and meat products [2] and congenital transmission from *T. gondii* infected pregnant women [4] [5] and blood transfusion/organ transplantation [6] [7]. Generally, the primary infection is asymptomatic or with mild flu-like symptoms in immune competent host, but can be fatal and severe in immune compromised individual and fetus bearing pregnant women [8].

T. gondii is critical in a sense that it can evade the immune system after acute infection and thereby undergoes developmental switching from fast replicating tachyzoite to slow replicating dormant bradyzoite preferentially in skeletal muscle and brain [9] [10]. This transformation from one parasite stage to another establishes chronic infection. As the parasite can infect any cells, it can affect other organs including heart [11], eyes [12], kidney [13] and liver [14]. Liver is an important organ where the entire metabolism e.g. carbohydrate, lipids, proteins, detoxification of xenobiotics and drugs takes place [15]. Many studies show that the parasite causes a number of pathological changes in liver including hepatitis, granuloma hepatomegaly and necrosis [14]. Furthermore, Ustun and colleagues has shown that *T. gondii* infection can be associated with liver cirrhosis [16]. These data nevertheless confirm the existence of hepatic toxoplasmosis. It has to be stressed that understanding of host parasite interaction is important for disease pathogenesis and designing new drugs. Recently, He J-J and colleagues has performed transcriptome and proteome analysis of *T. gondii* infected mouse liver to understand the impact of infection on host liver both at RNA and protein level [17] [18]. The authors identified differentially regulated genes (n = 2758) and proteins (n = 301) including up-and down-regulated genes and proteins in *T. gondii* infected mouse liver compared to non-infected one [17] [18]. However, one of the major limitations of the studies was to overlook the correlation of gene expression at both mRNA and protein level. This is important, because the entire transcript at RNA level does not participate in protein synthesis through translation which suggests the presence of epigenetic regulation at transcription or translation level. Therefore, this study has been designed to integrate both transcriptome and proteome data set of *T. gondii* infected mouse liver for identifying the genes those are regulated as same fashion

in both transcription and translation. Herein, we have integrated whole transcriptome shotgun sequencing (RNAseq) and tandem mass spectrometry (LC-MS/MS) proteomics of *T. gondii* infected mouse liver to get better understanding of host-parasite interaction and molecular mechanism of disease pathogenesis. The integrated analysis of transcriptomics and proteomics data merges large number of RNA transcripts with relatively less number of proteins to find out common candidates by cross matching the sequence identifier. The outcome of this integrated technology helps further analysis on gene ontology to discover accurate biological role of selected and common transcript/proteins.

A large number of cellular processes are mediated by physical interactions among proteins such as, signal transduction, enzyme activity, and post-translational modification. A protein-protein interaction (PPI) network has a small number of highly connected protein nodes (known as hubs) and many poorly connected nodes. These hub proteins are the most important for survival and reproduction of that particular organism. They may function as effector molecules for disease pathogenesis, diagnostic marker and drug target. As homology modeling of these hub proteins were also analyzed in this study, the information might be useful to get a rough idea where the alpha carbons of key residues sit the folded protein. They can guide site-directed mutagenesis experiments, or hypotheses about structure-function relationships. Even within the pharmaceutical industry homology modeling can be valuable in structure-based drug discovery and drug design.

All of these analyses were done on integrated transcriptomic and proteomic data. So, findings of our study may provide useful insights of pathogenesis of *T. gondii* infection and host-parasite interaction.

2. Methods and Materials

2.1. Retrieval of Data Set

Raw data files of transcriptome and proteome analyses of *T. gondii* infected mouse liver were retrieved separately from online database deposited from the study of He J-J and colleagues [17] [18]. Briefly, in these studies BLALB/c mice and PYS strain were used as host and *T. gondii* parasite respectively. Three mice were either infected with *T. gondii* tachyzoite (n = 200) and/or were treated with PBS for non-infected control. Liver tissues were collected from 6 days post infected and control mice for experimental analysis. RNA sequencing and LC-MS analysis were performed with the infected and non-infected liver tissue to determine gene expression pattern at RNA level and protein profiling at protein level. From the raw data set, differentially regulated genes and proteins files were sorted and used for further analysis in this study. Outline of the whole procedure is shown in **Figure 1**.

2.2. Analysis of Differentially Expressed Genes and Proteins

Venn analysis was performed with differentially expressed genes and proteins to

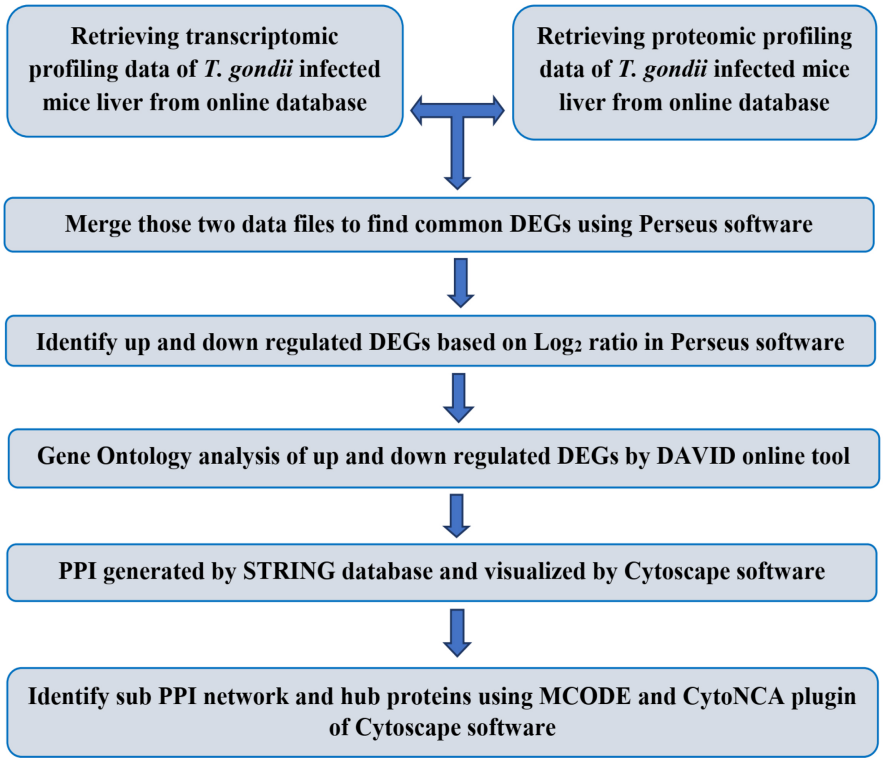

Figure 1. A schematic representation of the workflow for analyzing transcriptome and proteome data. Abbreviations: DEG, Differentially Expressed Gene; DEP, differentially expressed b proteins; DAVID, Database for Annotation, Visualization and Integrated Discovery; PPI, Protein-Protein Interaction; STRING, Search Tool for the Retrieval of Interacting Genes/Proteins; CytoNCA, A Cytoscape apps for network centrality analysis; MCODE, a cytoscape apps for molecular complex detection.

find out the common transcripts those are translated into proteins using Venn diagram online software of the VIB/UGent (http://bioinformatics.psb.ugent.be/webtools/Venn/). Transcript those translated into proteins was further analyzed in pursues software (http://www.coxdocs.org/doku.php?id=perseus:start) to find out up and down-regulated DEGs/DEPs. The program provided a scatter diagram which clearly showed these two groups separately.

GO analysis was performed on 159 DEGs/DEPs to study the global biological changes in liver function after *T. gondii* infection by using DAVID (Data-base for Annotation, Visualization, and Integrated Discovery) tool. The tool was used for gene ontology search to investigate biological processes, cellular components and molecular functions. GO terms having an EASE score (a modified Fisher Exact P-Value) less than 0.05 and Count (number of DEGs/DEPs involved in any GO terms) equal or greater than 5 were considered.

Differentially expressed up and down regulated genes/proteins were also analyzed through Cytoscape 64-bit program for identification of their association on different pathways including biological process, cellular process and molecular function.

2.3. Analysis of Protein-Protein Interaction

Protein-protein interaction network was also prepared by using both STRING and Cytoscape program. Protein-protein interactions were generated in STRING and subsequently the interaction network was imported into Cytoscape software for visualization and further analysis. STRING parameters were kept as it is (minimum required interaction score (medium confidence) was 0.4 and as maximum number of interactors, only query proteins being displayed. Average local clustering coefficient of this PPI was 0.754 and PPI enrichment p-value was less than 1.0e−16. These proteins were found to interact among themselves than expected.

2.4. Analysis of mRNA-Protein Stability

Data containing protein and mRNA copy numbers, half-lives, transcription rate and translation rate constants in mouse fibroblasts (NIH3T3) was downloaded from online repository [19]. In this study they used amino acids and a nucleoside analogue 4-thiouridine (4sU) for labelling to measure simultaneously protein and mRNA turnover in a population of exponentially growing non-synchronized NIH3T3 mouse fibroblasts. They quantified proteins by liquid chromatography and online tandem mass spectrometry (LC-MS/MS) and identified 84,676 peptide sequences. Later they assigned them to 6445 unique proteins (false discovery rate, 1% at the peptide and protein level). After pulse labelling, they fractionated RNA samples into the newly synthesized and pre-existing fractions and analyzed them by mRNA sequencing and quantified by mapping reads to their exonic region. They calculated mRNA half-lives based on the ratios of newly synthesized RNA/total RNA ratio and the pre-existing RNA/total RNA ratio. On the other hand, proteins were five times more stable than mRNAs. Notably, they did not find any correlation between protein and mRNA half-lives (R2 = 0.02). So, to investigate the experimental noise they performed a second independent large-scale experiment and measured mRNA and protein levels and their half-lives again. The overall correlation of half-lives and levels between both replicates was good. They deposited the raw data to publicly available online database.

3. Results

Proteotranscriptomics approach has not been utilized to its full potential to study the host-pathogen interactions. Here, we integrated transcriptomic and proteomic approaches to identify factors involved in the pathogenesis of *Toxoplasma gondii* (*T. gondii*) infected mouse liver. Recently, He J-J *et al*. studied transcriptome and proteome of mouse liver before and after *T. gondii* infection using RNA sequencing [17] and liquid chromatography-mass spectrometric (LC-MS/MS) technique [18]. The authors deposited the raw data to publicly available online database. Herein, raw data files of transcriptome and proteome of *T. gondii* infected mouse liver were retrieved separately and used for further analysis to integrate both approaches for searching novel factors involving dis-

ease pathogenesis and drug target.

3.1. Identification of Common Differentially Expressed Genes/Proteins

From transcriptome analysis of *T. gondii* infected mouse liver, 18,000 transcripts were identified at RNA level [17]. Among them 2758 transcripts were differentially expressed. On the other hand, proteome analysis of *T. gondii* infected mouse liver revealed 3700 proteins of which 301 were differentially expressed [18].

After analyzing 2758 differentially expressed genes (DEGs) and 301 differentially expressed proteins (DEPs), common DEGs and DEPs expressed in both transcriptome and proteome level were identified by merging two datasets in Perseus software. Results revealed that 159 DEGs/DEPs were expressed at both RNA and protein level as shown in **Figure 2(a)**. Our data also showed that 2599

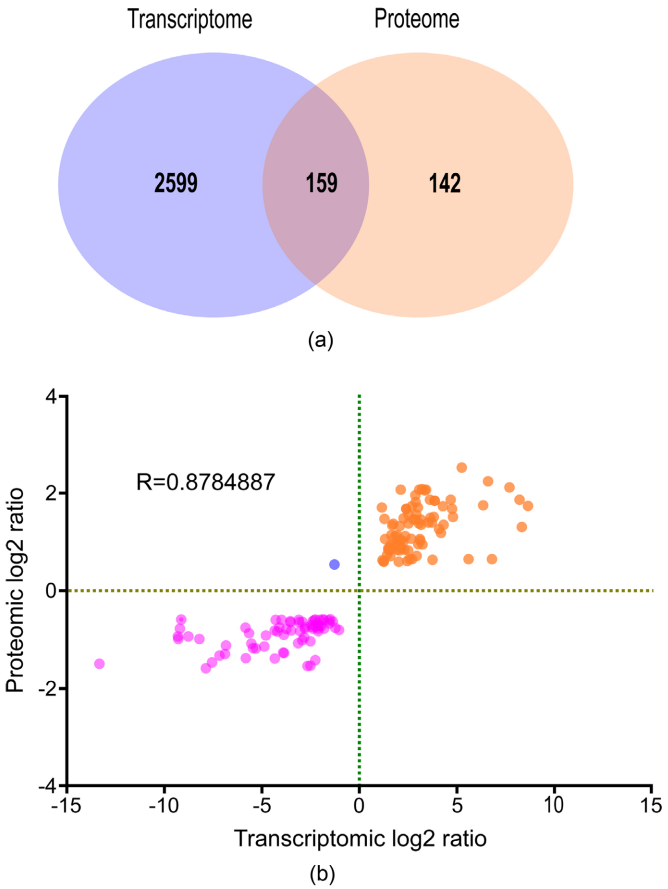

Figure 2. (a) Venn diagram of differentially expressed genes/proteins of *T. gondii* infected mouse liver. Transcriptomic analysis of *T. gondii* infected mice liver identified 2758 DEGs and proteomic analysis of infected mouse liver identified 301 DEPs in *T. gondii* infected mice liver. After analysis 159 DEGs/DEPs were found at both RNA and protein level. (b) Scatter diagram of common 159 differentially regulated genes/proteins. Perseus software was used to create this figure using transcriptomic Log_2 and proteomic Log_2 data of 159 DEGs/DEPs.

DEGs were only found at RNA level whereas 142 DEPs were found at protein level. List of common 159 DEGs/DEPs are shown in supplementary Table S1.

3.2. Identification of Up and Down-Regulated Genes/Proteins

Among these 159 differentially expressed genes/proteins, 86 were found to be up-regulated while 72 were down-regulated (Supplementary Table S2 and Table S3, respectively) using Perseus software. These DEGs/DEPs were used to create a scatter plot with four quadrants (Figure 2(b)) where quadrant I revealed 86 DEGs/DEPs (orange) which had increased level of expression that indicates higher transcriptomic and proteomic log2 value. In quadrant III, there were 72 DEGs/DEPs (purple) which had low transcriptomic and proteomic log2 value. Quadrant II represented one single DEGs/DEPs (blue) which was considered as mixed expression and deviated from its principle. From this figure it was also found that no DEGs/DEPs had fallen into quadrant IV.

3.3. Gene Ontology (GO) Analysis of Up-Regulated Genes/Proteins

GO analysis was performed on 159 DEGs/DEPs to study the global biological changes in liver function after *T. gondii* infection by using DAVID. This reveals that 86 up-regulated genes/proteins were associated with 17 biological processes, 16 cellular components and 10 molecular functions (Supplementary Table S4). Different GO terms and its participating DEGs/DEPs number were used to prepare Figures 3(a)-(c). Among 17 biological processes top four processes (Immune System Process, Innate Immune Response, Cellular Response to Interferon-beta and Adaptive Immune Response) have significant FDR value and largest number of genes enriched. From GO analysis it was also found out that the up-regulated gene products mainly enriched in the extracellular exosome (44), blood micro-particle (14), extracellular space (25) and extracellular region (24). These were the top 4 terms of GO cellular component having significant FDR value. Cytoplasm and membrane were two other cellular components having large number of DEGs/DEPs enriched (38 and 37 respectively) but their FDR value was high. So, they were not considered as enriched terms. Similarly, Figure 3(c) revealed that "GTPase activity" (FDR = 0.0029), "GTP binding" (FDR = 0.034), "Serine-type endopeptidase inhibitor activity" (FDR = 0.196) and "Peptidase inhibitor activity" (FDR = 0.196) were the most enriched term with 9, 10, 6 and 6 genes hits respectively.

3.4. Gene Ontology (GO) Analysis of Down-Regulated Genes/Proteins

72 down regulated DEGs/DEPs were found to be associated with 7 biological pathways, 10 cellular components and 15 molecular functions (Figures 4(a)-(c)). GO terms along with their associated genes were listed in supplementary Table S5. Among 7 biological pathways, oxidation-reduction process, metabolic process, lipid metabolic process and transport were the top four terms having

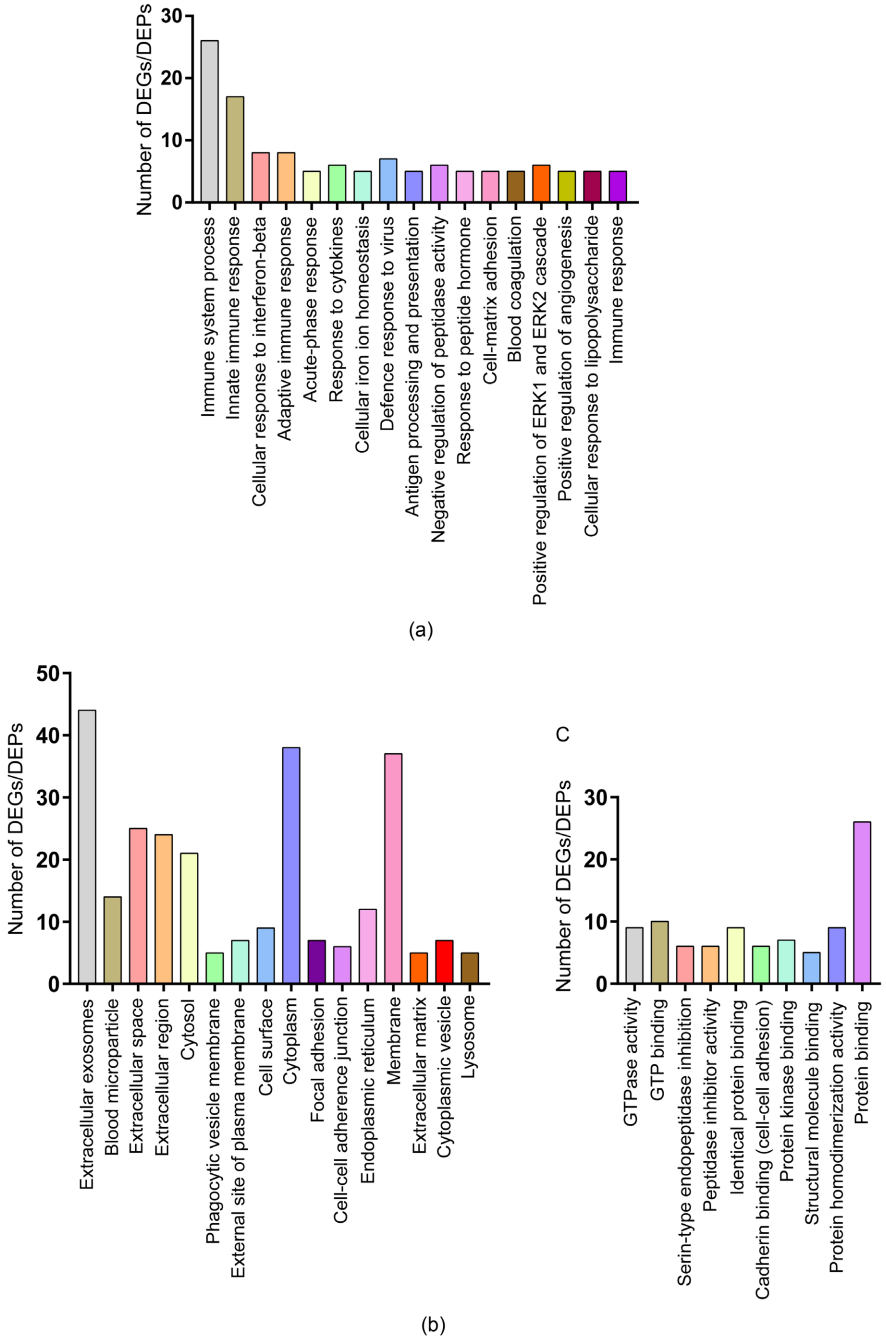

Figure 3. (a) Gene ontology for biological process analysis of up-regulated genes/proteins. (b) Gene ontology for cellular component (CC) annotation of up-regulated genes/proteins. (c) Gene ontology molecular function (MF) annotation of up-regulated genes/proteins.

the largest number of genes enriched. Down-regulated cellular component and associated differentially expressed genes/proteins were shown in **Figure 4(b)**. This figure revealed that the down-regulated gene products mainly located in the Organelle Membrane (12), Mitochondria (26), Endoplasmic Reticulum Membrane (17) and Intracellular Membrane-bounded Organelle (17). These were the top four terms of GO cellular component having significant FDR value.

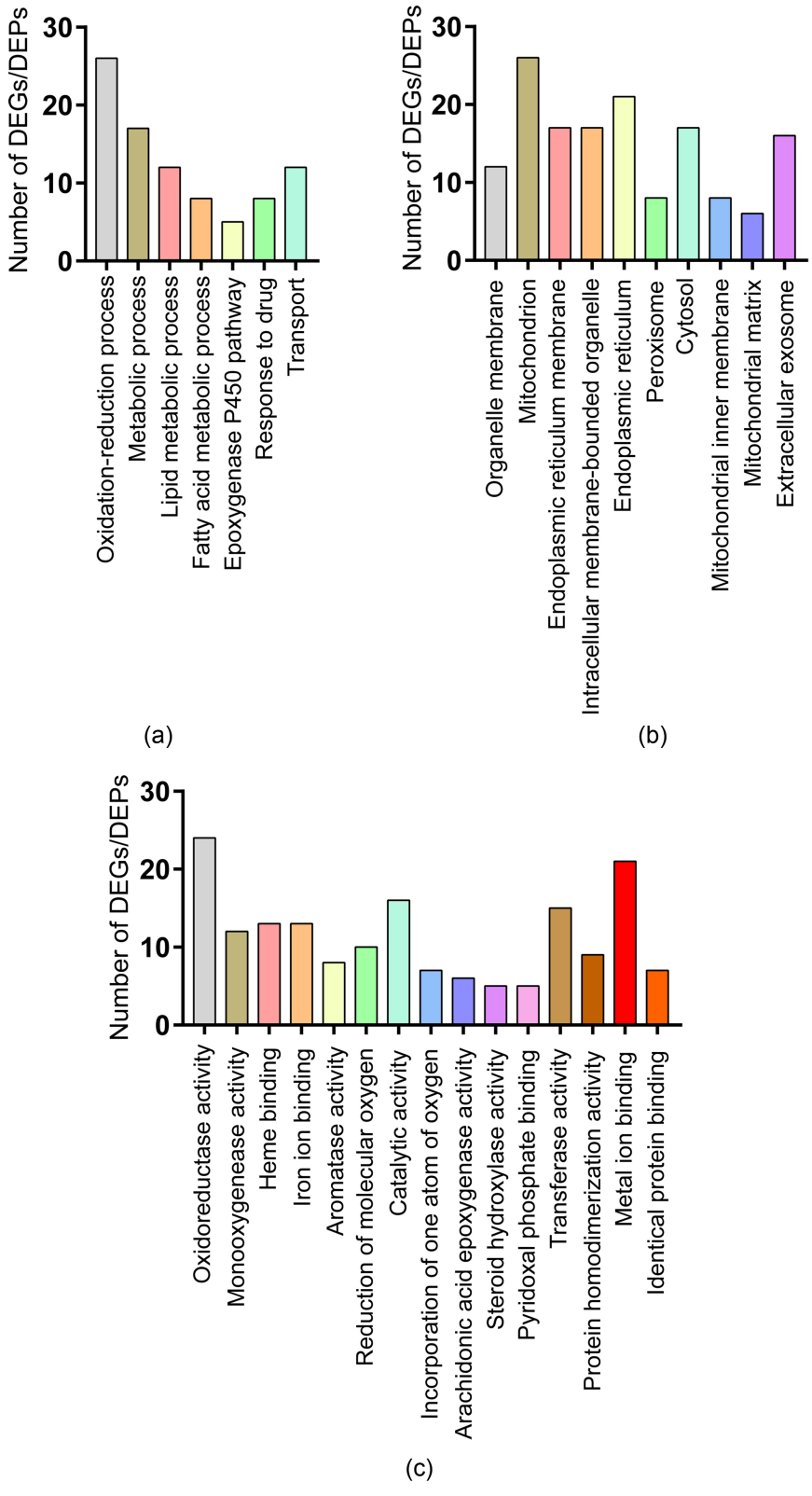

Figure 4. (a) Gene ontology for biological process analysis of down-regulated genes/proteins. (b) Gene ontology for cellular component (CC) annotation of down-regulated genes/proteins. (c) Gene ontology for molecular function (MF) annotation of down-regulated genes/proteins.

From this analysis it was also found out that Oxidoreductase activity, Monooxygenase activity, Heme binding and Catalytic activity were the most enriched term with 24, 12, 13 and 16 genes hits respectively (**Figure 4(c)**).

3.5. Gene Ontology Analysis of Unique Differentially Expressed Transcript (DETs) and Differentially Expressed Proteins (DEPs)

From the **Figure 2(a)** it was found that 2599 differentially expressed transcripts didn't take part in translation. That's why these 2599 DETs and 142 DEPs were considered as unique. According to DAVID tool, 318 biological processes were found to be associated with 2599 DETs. Top 20 GO terms were shown in supplementary **Figure 1(a)**. 203 DETs fell into the category of "Oxidation-reduction process", whose FDR value was 5.26E−40. The category of "Immune system process" (FDR = 3.86E−24), "Inflammatory response" (FDR = 1.09E−18), "Metabolic process" (FDR = 6.39E−18) were associated with 120, 103, 123 DETs respectively. These were the significantly enriched biological processes with the largest number of DETs hits. Similarly, GO annotation also revealed that 18 biological processes were associated with 142 differentially expressed proteins (Supplementary **Figure S1(b)**). According to the supplementary **Figure S1(b)**, DEPs were associated with "Protein folding" (FDR = 0.011936) whereas, 14 DEPs with "Translation" (FDR = 0.026348). These were the significantly enriched GO terms with the largest number of DEPs hits. 22 DEPs fell into the category of "Transport" (FDR = 52.771). In spite of associating with large number of DEPs this GO term was not considered as significant due to its FDR value.

3.6. Protein-Protein Interaction (PPI) Analysis of Common DEPs

From gene ontology annotation it was found that immune system process is the most significantly enriched up-regulated biological process and oxidation-reduction process is the most significant down-regulated biological process in *T. gondii* infection. Protein-protein interaction (PPI) network of DEPs associated with these biological processes (immune system process and oxidation-reduction process) was generated by STRING (Search Tool for the Retrieval of Interacting Genes/Proteins) database. This data then imported into Cytoscape (https://cytoscape.org/) software to visualize the protein interaction relationship network and to analyze significant clusters and hub proteins. Data showed that Immune system processes were mediated by 26 DEPs in mouse. According to DAVID output this was the top-most biological process having a significant FDR value (5.75E−21) which was up-regulated after *T. gondii* infection. Although GO analysis showed that 26 up-regulated proteins were involved in immune system process, after generating a PPI in STRING it was found that one protein, Pml, does not interact with any other protein. So, after filtering out disconnected protein, a PPI network containing 76 interactions for a total of 25 DEPs was generated as shown in **Figure 5(a)**. Such enrichment (25 DEPs had 76

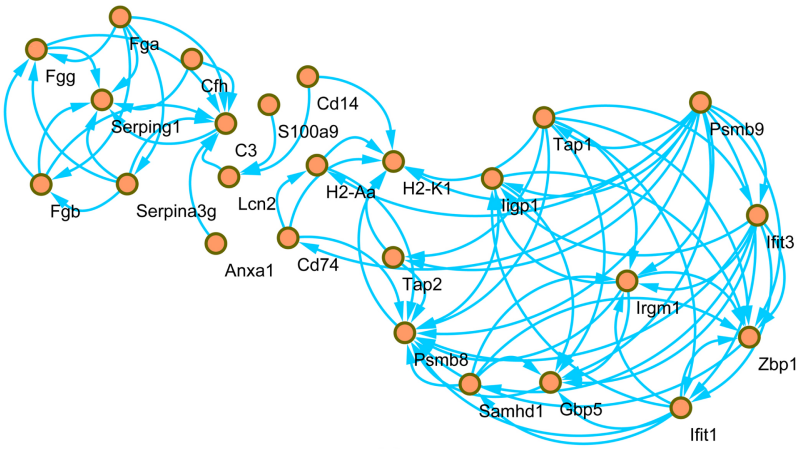
Fga
Fgg
Cfh
Cd14
Serping1
S100a9
C3
Tap1
Psmb9
H2-Aa
H2-K1
Iigp1
Ifit3
Fgb
Serpina3g
Lcn2
Anxa1
Cd74
Tap2
Irgm1
Psmb8
Zbp1
Samhd1
Gbp5
Ifit1

(a)

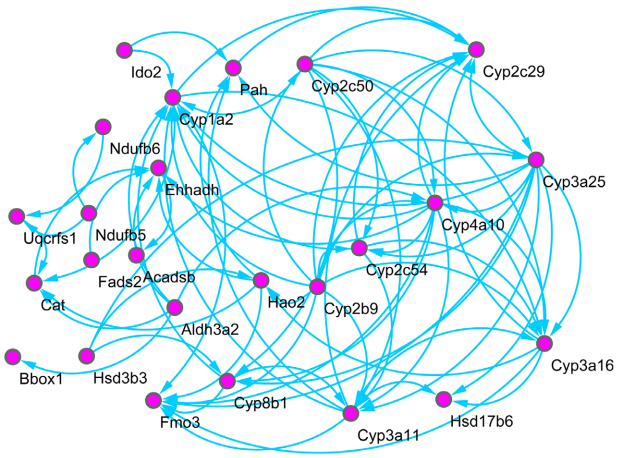
Ido2
Pah
Cyp2c50
Cyp2c29
Cyp1a2
Ndufb6
Cyp3a25
Ehhadh
Cyp4a10
Uqcrfs1
Ndufb5
Cyp2c54
Fads2
Acadsb
Cat
Hao2
Cyp2b9
Aldh3a2
Cyp3a16
Bbox1
Hsd3b3
Cyp8b1
Fmo3
Cyp3a11
Hsd17b6

(b)

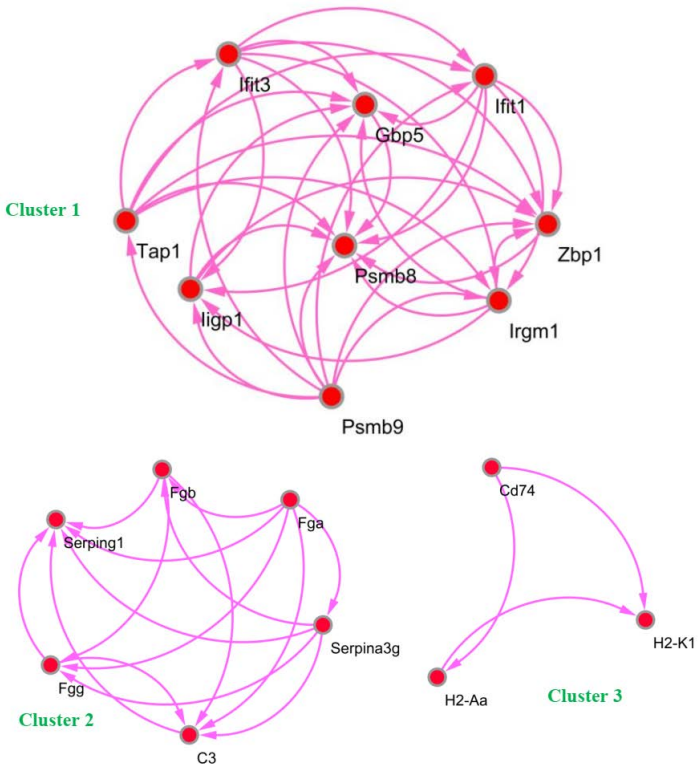
Cluster 1
Ifit3
Ifit1
Gbp5
Tap1
Zbp1
Psmb8
Iigp1
Irgm1
Psmb9
Cluster 2
Fgb
Fga
Serping1
Serpina3g
Fgg
C3
Cd74
H2-K1
H2-Aa
Cluster 3

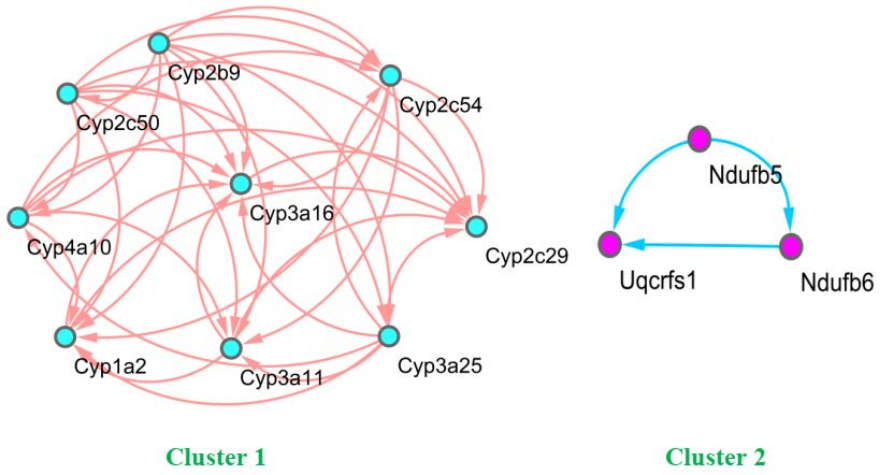

Figure 5. (a) Protein-protein interaction (PPI) among up-regulated proteins involved in immune system process. Nodes represent proteins (brown color) while, blue arrow represents interaction between proteins. (b) Protein-protein interaction (PPI) among down-regulated proteins involved in oxidation-reduction process. Nodes (purple color) represent proteins while, blue arrow represents interaction between proteins.

interactions) suggested that the proteins were at least partially biologically connected, as a group. 25 DEPs which were involved in this PPI, were Ifit3, Serping1, Fgb, Fga, Samhd1, C3, Serpina3g, Cd74, Lcn2, Irgm1, Gbp2b, Tap1, S100a9, Tap2, Zbp1, Psmb9, Anxa1, Psmb8, Cfh, Cd14, H2-K1, Fgg, Ifit1 and H2-Aa. Gene ontology analysis of 72 down-regulated DEPs revealed that the top most biological process was oxidation-reduction process having a significant FDR value (2.60E−17). Analysis result showed that 26 DEPs were involved in this process. A protein-protein interaction (PPI) among these 26 proteins was generated in STRING database and imported the data into Cytoscape software for visualization. Among these 26 DEGs/DEPs, Me1 did not interact with other proteins. Figure 5(b) was designed after filtering out this disconnected protein. Default parameters were used as before. A PPI network containing 79 interactions for a total of 25 DEPs was generated in Cytoscape software. Average local clustering coefficient of this interaction is 0.615 and PPI enrichment p-value is less than 1.0e−16. This indicated that these proteins interacted among themselves than expected. 25 DEPs of this PPI were Fmo3, Cyp3a16, Cyp2b9, Cyp8b1, Cyp3a11, Hsd17b6, Bbox1, Cyp2c29, Pah, Cat, Ido2, Fads2, Ndufb6, Ndufb5, Hsd3b3, Ehhadh, Uqcrfs1, Cyp4a10, Cyp2c50, Cyp3a25, Cyp2c54, Cyp1a2, Acadsb, Hao2, and Aldh3a2.

3.7. Determination of mRNA-Protein Stability Using Half Life

Snapshot analysis of mRNA and protein levels alone cannot provide sufficient information to understand the dynamic nature of gene expression comprehensively. Of note the impact of mRNA and protein half-lives on their respective abundance may provide important insight into the regulatory pattern. We took advantage of the mRNA and protein half-lives datasets in moue fibroblast cells

from Bjorn Schwanhausser *et al.* In brief, the authors quantify cellular mRNA and protein expression levels and turnover in parallel in a population of unperturbed moue fibroblast cells by Pulse labelling to determine mRNA and protein half-lives [19].

Among the 159 common DEGs/DEPs which were identified in this current study, only 51 DEGs/DEPs were found to be matched from the half-life retrieved data. Again, among these 51 DEGs/DEPs, 31 had known stability according to retrieved data. These 31 DEGs/DEPs and their stability were enlisted in **Table 1**. Using these 31 DEGs/DEPs a scatter plot was generated for better understanding by using ggplot package of R programming language which was shown in **Figure 6**. Identification of the stability was based on half-lives of a particular gene on its mRNA and protein level. Intestinally, the hub-protein Tap1 showed higher mRNA and protein half-lives implying that hub-proteins may have higher mRNA and protein stability to carry out biological functions.

4. Discussion

Study of host-pathogen interaction is important for understanding the disease pathogenesis and drug treatment. Recently, He J-J and colleagues did transcriptome and proteome analysis separately on *T. gondii* PYS strain infected BALB/c

Table 1. List of common DEGs/DEPs along with their stability.

mRNA Stable, Protein Stable (Quadrant I)	mRNA Stable, Protein Unstable (Quadrant II)	mRNA Unstable, Protein Unstable (Quadrant III)	mRNA Unstable, Protein Stable (Quadrant IV)
Gbp4	Cd74	Cd14	Ifit1
Samhd1	Stat3	Eif1a	Lactb2
Aldoa	Cp	Hmox1	
Arhgdib	Fth1		
Dpp9	Pml		
G6pdx	Xdh		
Gbp2	Cat		
Mvp	Fads2		
Tap1	Fkbp8		
Pgm2	Ndufb5		
Abcd3	Oat		
Acadsb			
Atp5j			
Me1			
Ugp			

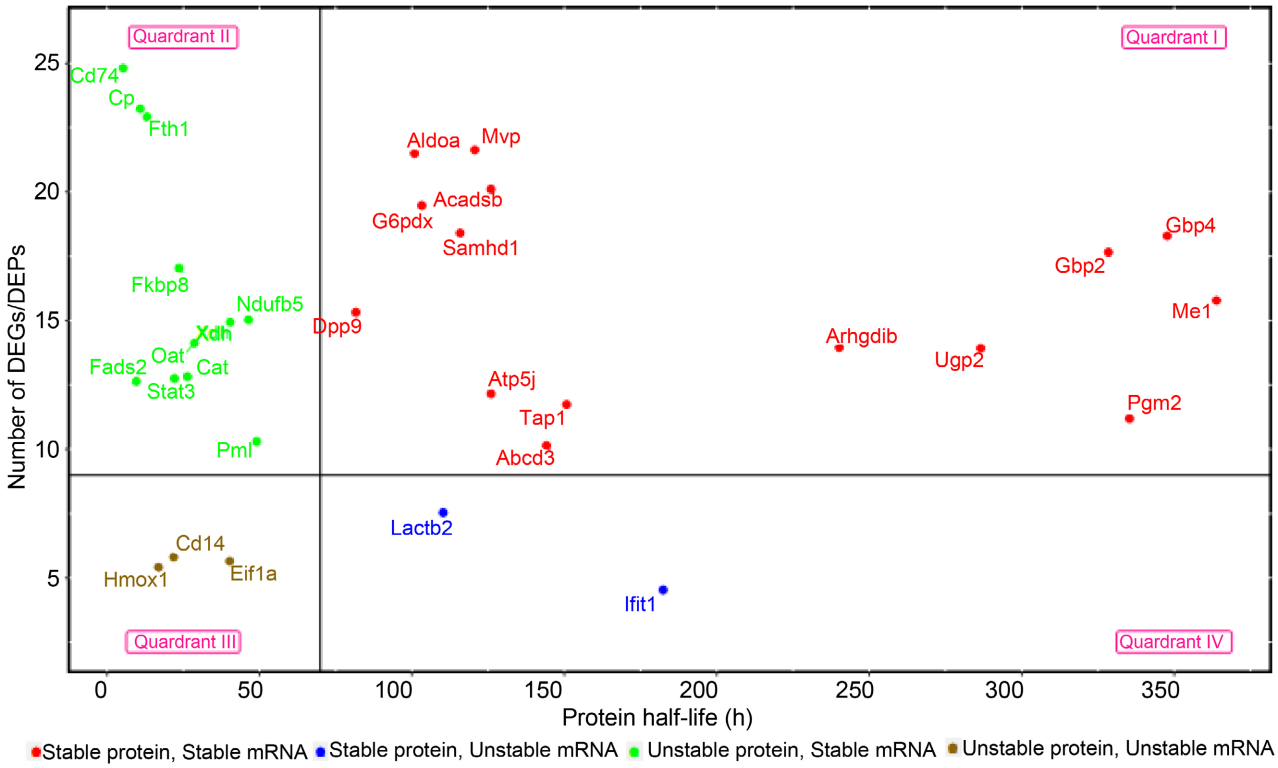

Figure 6. mRNA-Protein stability confirm by half-life: A scatter plot showing stability of common DEGs/DEPs. 15 genes fell into quadrant I whose encoded mRNAs and proteins both were stable. Quadrant II had 11 genes whose encoded mRNAs were stable and proteins were unstable. 3 genes fell into quadrant III whose encoded mRNAs and proteins both were unstable and lastly, quadrant IV had 2 genes whose encoded mRNAs were unstable but proteins were stable.

mice liver. In this study, raw date of transcriptome and proteome from *T. gondii* infected and uninfected mouse liver tissues were further analyzed through integrated proteotranscriptomic approaches. It has to be stressed that liver is an important organ that perform multiple task in the body. For example, 1) It can act as a storage site of glycogen, vitamins and minerals; 2) It can act as a house of metabolism of carbohydrate, proteins fat and drugs; 3) It helps for the synthesis and excretion of bile acid, bilirubin, cholesterol, etc. Besides, after acute infection *T. gondii* can undergoes stage conversion from fast replicating tachyzoite to slow replicating bradyzoite not only in brain and skeletal muscle but also in liver, eyes etc. Thus, *T. gondii*may causes liver cirrhosis and inflammation. Therefore, study of transcriptome and proteome of *T. gondii* infected mouse liver might help to understand the mechanism on the impact of the parasite on liver function. Some previous studies on serological, biochemical and direct detection of *T. gondii* have revealed that *T. gondii* infection plays an important role in liver pathologies [16] [20]. However, mechanism of how *T. gondii* establishes hepatic infection remains unclear.

Transcriptome of T. gondii infected and non-infected mouse liver revealed 2758 differentially regulated genes and 301 differentially regulated proteins, among them 159 differentially expressed genes (DEGs) were identified as common and those were translated into differentially expressed proteins (DEPs).

This data suggests that all of the differentially expressed genes are not completely translated into proteins. The possible reasons could be: 1) There might be some unstable RNA that does not participate in protein synthesis 2) Among these, even some protein may degrade quickly therefore not found at the time of translation.

After infection *T. gondii* developed strategies to manipulate host immune system, energy metabolism, and signaling by inducing host cell gene transcription [21]. Gene ontology analysis of these 159 DEGs/DEPs showed that immune response, extracellular exosome, blood micro-particle, extracellular space, GTPase activity, peptidase inhibitor activity and identical protein binding activity become up-regulated while, oxidation-reduction, fatty acid metabolism, lipid metabolism, organelle membrane, mitochondria, oxidoreductase activity, heme binding and monooxygenase activity become down-regulated during the early stage of *T. gondii* infection. In a previous study on proteomic profiling on mouse liver during acute toxoplasmosis it was suggested that endosome and proteolysis activity become upregulated after *T. gondii* infection [18] while, our results demonstrated that extracellular exosome and peptidase inhibitor activity become up-regulated in this parasitic infection. This discrepancy between the results may be attributed to the use of different tools. Regardless, up-regulation of immune response related terms and down-regulation of different metabolic pathways are, overall, consistent with previous transcriptomic and proteomic reports in previous studies [22] [23] [24].

Understanding PPI is essential for understanding molecular and cellular mechanism, in healthy and diseased states of an organism. Consequently, this knowledge can be translated into effective diagnostic and therapeutic strategies such as drug or vaccine development. Here, proteins involved in most significantly enriched up-regulated (Immune system process) and down-regulated (Oxidation-reduction process) biological process were used to generate PPI.

Investigation of the modular properties of protein–protein interaction (PPI) networks can facilitate further discovery of the underlying molecular interaction mechanisms that drive cell response under specific conditions, such as drug treatment [25]. In some previous studies interaction networks were used to predict gene function, to identify novel disease-related genes and to understand the overlapping association across disease phenotypes [26] [27]. Recently, computational approaches have been used to build topological clusters as functional modules in PPI networks [28].

MCODE was used as discovery tools to further analyze the network and extract sub network from the whole PPI. Based on the topological structure three densely connected clusters were found from the whole PPI of proteins involved in immune system process (**Figure 5**). Cluster 1 proteins had high score that includes 9 nodes and 34 edges. Nodes are following-Ifit3, Ifit1, Iigp1, Zbp1, Psmb8, Psmb9, Tap1, Gbp2b, Irgm1proteins. Based on the importance connectivity of these 9 proteins only three (Psmb8, Psmb9 and Tap1) were identified as hub

protein by CytoNCA application. Psmb8 has established well known association with the etiology and pathology of toxoplasmosis [29].

The proteasome is a multi-catalytic proteinase complex which is characterized by its ability to cleave peptides with Arginine, Phenyl alanine, Tyrosine, Leucine, and Glutamate adjacent to the leaving group at neutral or slightly basic pH. The proteasome has an ATP-dependent proteolytic activity. Psmb8 (proteasome subunit beta type-8) subunit belongs to the peptidase T1B family (276 amino acid) and is required for adipocyte differentiation. This subunit is involved in antigen processing to generate class I binding peptides and in the inflammatory response pathway. A previous study showed that *T. gondii* infection induce the expression of Psmb8 mRNA in antigen presenting cell (APC) and increase the capacity of APC to induce the production of IFN-γby antigen-specific CD8+ T cells [29]. *In vitro* infection of a dendritic cell (DC) cell line with *T. gondii* can also induce the expression of Psmb8and resulted in enhanced proteasome proteolytic activity. In their study they also observed that mice lacking Psmb8were also shown to be highly susceptible to infection with *T. gondii* and showed a reduced number of functional CD8+ T cells.

Another subunit, Psmb 9, belongs to the peptidase T1B family (219 amino acid). It is involved in antigen processing to generate class I binding peptides and contributes to (nuclear factor kappa-beta 1A (NFKB1A) degradation and subsequently NFKB1 generation. Luisa Möhle and colleagues identified a strong increase of mRNA expression for the immunoproteasome subunits Psmb 9 (LMP 2) and Psmb 8 (LMP7) in whole-brain RNA from *T. gondii* infected mice [30].

TAP 1 (Antigen peptide transporter 1) belongs to the ABC transporter superfamily (ABCB family) and MHC peptide exporter subfamily (724 amino acid). They are involved in the transport of antigens from the cytoplasm to the endoplasmic reticulum for association with major histocompatibility complex I (MHC class I) molecules. It also acts as a molecular scaffold for the final stage of MHC class I folding, namely the binding of peptide. Nascent MHC class I molecules associate with TAP via tapasin based on similarity. Goldszmid RS and colleagues revealed that TAP 1 plays an important role in the induction of interferon-gamma-producing natural killer (NK) cells and demonstrate that NK cell licensing can influence host resistance to *T. gondii* infection through its effect on cytokine production in addition to its role in cytotoxicity. So, it can be said that TAP-1 indirectly regulates CD4+ T cell priming in *Toxoplasma gondii* infection by controlling NK cell IFN-gamma production [31]. Furthermore, six other proteins from cluster one including Ifit3, Ifit1, Iigp1, Zbp1, Gbp2b and Irgm1 were also associated with up-regulating immune response after *T. gondii* infection. Though in my present study Ifit3 and Ifit1 were found to be significantly upregulated during acute *T. gondii* infection, there is no such study which show the association of Ifit3 and Ifit1with *T. gondii* infection. Association of rest of the 4 proteins with toxoplasmosis was found previously.

Z-DNA binding protein 1 (ZBP1) is one of the most abundant host transcripts

during acute and chronic *T. gondii* infection. In one study, Pittman KJ and colleagues determined that ZBP1 functions to control *T. gondii* growth thus minimizing the infection (Pittman *et al*., 2016). Another study showed that Zbp1 can initiate innate immune responses by binding cytosolic DNA (Wang *et al*., 2008). However, there are few reports regarding the contribution of Zbp1 to NF-κ-beta activation in the spleen of mice infected by *T. gondii* [32].

IIGP1 (Interferon-inducible GTPase1) is essential for interferon-γ-induced cell-autonomous immunity against *T. gondii* in mice, but the mechanism of resistance is poorly understood. In a study Sascha Martens and colleagues showed that IIGP1 accumulate at live *T. gondii* containing vacuoles in a GTP-dependent manner. After maturation-like process vesiculation of the parasitophorous vacuole membrane occurs. This culminates in disruption of the parasitophorous vacuole and finally of the parasite itself. They also found that over-expression of IIGP1 leads to accelerated vacuolar disruption while, targeted deletion of the IIGP1 gene results in partial loss of the IFN-γ-mediated *T. gondii* growth restriction in mouse astrocytes [33].

GBP2 (guanylate binding proteins) is also a GTPase protein which inhibits replication of *Toxoplasma gondii.* Some previous studies showed that murine GBP2 (mGBP2) is highly expressed in several cell types, including T and B cells after stimulation and revealed that mGBP2-deficient mice has a marked immune susceptibility to *T. gondii* [34]. So, it can be said that mGBP2 is an essential immune effector molecule mediating anti-parasitic resistance. IRGM1 proteins (immunity-related GTPases) provide an early defense mechanism in mice against the protozoal pathogen, *T. gondii.* IRGM knocked-out mice show striking susceptibility to *T. gondii* infection [35] [36]. Zbp1 can initiate innate immune responses by binding cytosolic DNA [37]. However, there are few reports regarding the contribution of Zbp1 to NF-κB activation in the spleen of mice infected by *T. gondii.*

By similar manner, 2 sub networks (significant clusters) were extracted using MCODE application from whole PPI of proteins which were involved in down-regulating oxidation-reduction process. Among 9 proteins (CYP3A16, CYP2C29, CYP1A2, CYP2C54, CYP3A25, CYP3A11, CYP2C50, CYP4A10, CYP2B9) of highly scored cluster 1 three proteins were identified as hub proteins by CytoNCA algorithm, which are following-CYP1A2, CYP4A10 and CYP3A25). Surprisingly, all of the proteins are members of cytochrome P450 superfamily of enzymes. The former application (MCODE) analyzes network based on topological structure, while the latter (CytoNCA) provides an estimate of functions based on gene annotations. Some previous studies also revealed the association of these down-regulated proteins with acute *T. gondii* infection in mouse liver [32].

Sub networks and hub proteins provide novel hypotheses for pathways involved in disease [38] [39]. They have some special biological properties, for example, they tend to be more essential than non-hub proteins [40] [41], they are

found to play a central role in modular organization of the protein interaction network [42] [43] and some studies indicate that hub proteins may also be evolutionarily conserved to a larger extent than non-hubs [43].

Investigation of the modular properties of protein-protein interaction (PPI) networks can facilitate further discovery of the underlying molecular interaction mechanisms that drive cell response under specific conditions, such as drug treatment [25]. In some previous studies interaction networks were used to predict gene function, to identify novel disease-related genes and to understand the overlapping association across disease phenotypes [27] [44]. Recently, computational approaches have been used to build topological clusters as functional modules in PPI networks [28].

The resulting hub proteins and functional clusters of my current study might be useful to reveal the pathological mechanism of *T. gondii* induced toxoplasmosis in host. Further investigation into these hub proteins elucidating their role in regulating immune system and oxidation-reduction process can be an interesting avenue of exploration and can be of help while designing drugs. They can also be used as bio-marker in the diagnostic field.

In this current study, structure prediction of these hub proteins was also done by homology modeling. Homology modeling has become a useful tool for the prediction of protein structure when only sequence data are available. Structural information is often more valuable than sequence alone for determining protein function, dynamics and interactions with ligands or other proteins. The "low-resolution" structure provided by homology modeling contains sufficient information about the spatial arrangement of important residues in the protein and may guide the design of new experiments, for example site-directed mutagenesis. Even within the pharmaceutical industry homology modeling can be valuable in structure-based drug discovery and drug design.

The resulting hub proteins and functional clusters of the current study might be useful to reveal the pathological mechanism of *T. gondii*-induced toxoplasmosis in the host. Further investigation into these hub proteins elucidating their role in regulating immune system and oxidation-reduction process can be an interesting avenue of exploration and can be of help while designing drugs. They can also be used as bio-marker in the diagnostic field.

5. Conclusion

In summary, the current study showed that how multi-OMICS integration approach can efficiently be used to elucidate the intricate molecular pathways that may contribute to the onset, development and progression of pathological condition during *Toxoplasma gondii* infection. The multi-OMICS integration of transcriptome and proteome lead to the identification of the effector molecules (hub proteins) that may potentially be of great importance and subsequently utilized in the in discovery of next-generation biomarker and the designing of efficient and rapid diagnosis of *Toxoplasma gondii* infections. Since the identified

hub-proteins showed differential expression pattern depending on the infection status, these proteins can be considered as ideal candidates for therapeutic and diagnostic targets. Further studies to pinpoint testing of identified effector molecules are to be performed. *In vitro* and *in vivo* study of these molecules would be interesting to confirm their functional activities and efficacy. Limitation of the study: Since *Toxoplasma gondii* is an intracellular protozoan parasite and causes mostly in asymptomatic infection in human. Due to primary asymptomatic infections and followed by self-recovery, proteome data from *T. gondii* infected clinical patients are not available and difficult to generate. Therefore, studying of *T. gondii* in mouse model could be insightful information for scientific arena.

Funding

No specific funding was allocated for this study.

Conflicts of Interest

The authors declare no conflict of interest for this publication.

References

[1] Flegr, J., Prandota, J., Sovičková, M. and Israili, Z.H. (2014) Toxoplasmosis—A Global Threat. Correlation of Latent Toxoplasmosis with Specific Disease Burden in a Set of 88 Countries. *PLoS ONE*, **9**, e90203. https://doi.org/10.1371/journal.pone.0090203

[2] Innes, E.A. and Innes, E.A. (2009) A Brief History and Overview of *Toxoplasma gondii*. *Zoonoses and Public Health*, **57**, 1-7. https://doi.org/10.1111/j.1863-2378.2009.01276.x

[3] Hussain, M.A., Stitt, V., Szabo, E.A. and Nelan, B. (2017) *Toxoplasma gondii* in the Food Supply. *Pathogens* (*Basel, Switzerland*), **6**, 21. https://doi.org/10.3390/pathogens6020021

[4] Pappas, G., Roussos, N. and Falagas, M.E. (2009) Toxoplasmosis Snapshots: Global Status of *Toxoplasma gondii* Seroprevalence and Implications for Pregnancy and Congenital Toxoplasmosis. *International Journal for Parasitology*, **39**, 1385-1394. https://doi.org/10.1016/j.ijpara.2009.04.003

[5] Andiappan, H., *et al.* (2014) Toxoplasma Infection in Pregnant Women: A Current Status in Songklanagarind Hospital, Southern Thailand. *Parasites & Vectors*, **7**, Article No. 239. https://doi.org/10.1186/1756-3305-7-239

[6] Räisänen, S. (1978) Toxoplasmosis Transmitted by Blood Transfusions. *Transfusion*, **18**, 329-332. https://doi.org/10.1046/j.1537-2995.1978.18378205142.x

[7] Wreghitt, T.G., *et al.*, (1989) Toxoplasmosis in Heart and Heart and Lung Transplant Recipients. *Journal of Clinical Pathology*, **42**, 194-199. https://doi.org/10.1136/jcp.42.2.194

[8] Montoya, J.G. and Liesenfeld, O. (2004) Toxoplasmosis. *The Lancet*, **363**, 1965-1976. https://doi.org/10.1016/S0140-6736(04)16412-X

[9] Dubey, J.P., Lindsay, D.S. and Speer, C.A. (1998) Structures of *Toxoplasma gondii* Tachyzoites, Bradyzoites, and Sporozoites and Biology and Development of Tissue Cysts. *Clinical Microbiology Reviews*, **11**, 267.

https://doi.org/10.1128/CMR.11.2.267

[10] Tenter, A.M., Heckeroth, A.R. and Weiss, L.M. (2000) *Toxoplasma gondii*: From Animals to Humans. *International Journal for Parasitology*, **30**, 1217-1258. https://doi.org/10.1016/S0020-7519(00)00124-7

[11] Manlio, *et al.* (2008) Temporal and Spatial Distribution of *Toxoplasma gondii* Differentiation into Bradyzoites and Tissue Cyst Formation *in Vivo*. *Infection and Immunity*, **76**, 3491-3501. https://doi.org/10.1128/IAI.00254-08

[12] Kadarisman, R.S., Marsetio, M. and Simangunsong, L.B. (1991) Visual Impairment and Blindness in Ocular. *The Southeast Asian Journal of Tropical Medicine and Public Health*, **9**, 99-101.

[13] Khurana, S. and Batra, N. (2016) Toxoplasmosis in Organ Transplant Recipients: Evaluation, Implication, and Prevention. *Tropical Parasitology*, **6**, 123-128. https://doi.org/10.4103/2229-5070.190814

[14] Alvarado-Esquivel, C., Torres-Berumen, J.L., Estrada-Martínez, S., Liesenfeld, O. and Mercado-Suarez, M.F. (2011) *Toxoplasma gondii* Infection and Liver Disease: A Case-Control Study in a Northern Mexican Population. *Parasites & Vectors*, **4**, 75. https://doi.org/10.1186/1756-3305-4-75

[15] Alamri, Z.Z. (2018) The Role of Liver in Metabolism: An Updated Review with Physiological Emphasis. *International Journal of Basic & Clinical Pharmacology*, **7**, 2271-2276. https://doi.org/10.18203/2319-2003.ijbcp20184211

[16] Ustun, S., Aksoy, U., Dagci, H. and Ersoz, G. (2004) Incidence of Toxoplasmosis in Patients with Cirrhosis. *World Journal of Gastroenterology*, **10**, 452-454. https://doi.org/10.3748/wjg.v10.i3.452

[17] He, J.-J. (2016) Transcriptomic Analysis of Mouse Liver Reveals a Potential Hepato-Enteric Pathogenic Mechanism in Acute *Toxoplasma gondii* Infection. *Parasites & Vectors*, **9**, 427. https://doi.org/10.1186/s13071-016-1716-x

[18] He, J.-J., Ma, J., Elsheikha, H.M., Song, H.-Q., Zhou, D.-H. and Zhu, X.-Q. (2016) Proteomic Profiling of Mouse Liver Following Acute *Toxoplasma gondii* Infection. *PLoS ONE*, **11**, e0152022. https://doi.org/10.1371/journal.pone.0152022

[19] Schwanhüusser, B., *et al.* (2011) Global Quantification of Mammalian Gene Expression Control. *Nature*, **473**, 337-342. https://doi.org/10.1038/nature10098

[20] Tiwari, I., Rolland, C.F., *et al.* (1982) Cholestatic Jaundice due to Toxoplasma Hepatitis. *Postgraduate Medical Journal*, **58**, 299-300. https://doi.org/10.1136/pgmj.58.679.299

[21] Blader, I.J. and Saeij, J.P. (2009) Communication between *Toxoplasma gondii* and Its Host: Impact on Parasite Growth, Development, Immune Evasion, and Virulence. *Apmis*, **117**, 458-476. https://doi.org/10.1111/j.1600-0463.2009.02453.x

[22] Nelson, M.M., *et al.* (2008) Modulation of the Host Cell Proteome by the Intracellular Apicomplexan Parasite *Toxoplasma gondii*. *Infection and Immunity*, **76**, 828-844. https://doi.org/10.1128/IAI.01115-07

[23] Zhou, D.-H., *et al.* (2013) Changes in the Proteomic Profiles of Mouse Brain after Infection with Cyst-Forming *Toxoplasma gondii*. *Parasites & Vectors*, **6**, Article No. 96. https://doi.org/10.1186/1756-3305-6-96

[24] Zhou, C.X., Elsheikha, H.M., Zhou, D.H., Liu, Q., Zhu, X.Q. and Suo, X. (2016) Dual Identification and Analysis of Differentially Expressed Transcripts of Porcine PK-15 Cells and *Toxoplasma gondii* during *in Vitro* Infection. *Frontiers in Microbiology*, **7**, 1-13. https://doi.org/10.3389/fmicb.2016.00721

[25] Iskar, M., *et al.* (2013) Characterization of Drug-Induced Transcriptional Modules:

Towards Drug Repositioning and Functional Understanding. *Molecular Systems Biology*, **9**, 662. https://doi.org/10.1038/msb.2013.20

[26] Lee, I., Lehner, B., Vavouri, T., Shin, J., Fraser, A.G. and Marcotte, E.M. (2010) Predicting Genetic Modifier Loci Using Functional Gene Networks. *Genome Research*, **20**, 1143-1153. https://doi.org/10.1101/gr.102749.109

[27] Sharan, R., Ulitsky, I. and Shamir, R. (2007) Network-Based Prediction of Protein Function. *Molecular Systems Biology*, **3**, 1-13. https://doi.org/10.1038/msb4100129

[28] Lu, Y., *et al.* (2019) Identification of Differentially Expressed Genes and Signaling Pathways Using Bioinformatics in Interstitial Lung Disease due to Tyrosine Kinase Inhibitors Targeting the Epidermal Growth Factor Receptor. *Investigational New Drugs*, **37**, 384-400. https://doi.org/10.1007/s10637-018-0664-z

[29] Tu, L., *et al.* (2009) Critical Role for the Immunoproteasome Subunit LMP7 in the Resistance of Mice to *Toxoplasma gondii* Infection. *European Journal of Immunology*, **39**, 3385-3394. https://doi.org/10.1002/eji.200839117

[30] Möhle, L., *et al.* (2016) Chronic *Toxoplasma gondii* Infection Enhances β-Amyloid Phagocytosis and Clearance by Recruited Monocytes. *Acta Neuropathologica Communications*, **4**, 25. https://doi.org/10.1186/s40478-016-0293-8

[31] Goldszmid, R.S., *et al.* (2007) TAP-1 Indirectly Regulates CD4+ T Cell Priming in *Toxoplasma gondii* Infection by Controlling NK Cell IFN-γ Production. *Journal of Experimental Medicine*, **204**, 2591-2602. https://doi.org/10.1084/jem.20070634

[32] He, J.J., *et al.* (2016) Transcriptomic Analysis of Global Changes in Cytokine Expression in Mouse Spleens Following Acute *Toxoplasma gondii* Infection. *Parasitology Research*, **115**, 703-712. https://doi.org/10.1007/s00436-015-4792-5

[33] Martens, S., *et al.* (2005) Disruption of *Toxoplasma gondii* Parasitophorous Vacuoles by the Mouse p47-Resistance GTPases. *PLOS Pathogens*, **1**, e24. https://doi.org/10.1371/journal.ppat.0010024

[34] Degrandi, D., *et al.* (2013) Murine Guanylate Binding Protein 2 (mGBP2) Controls *Toxoplasma gondii* Replication. *Proceedings of the National Academy of Sciences of the United States of America*, **110**, 294-299. https://doi.org/10.1073/pnas.1205635110

[35] Collazo, C.M., *et al.* (2001) Inactivation of LRG-47 and IRG-47 Reveals a Family of Interferon γ-Inducible Genes with Essential, Pathogen-Specific Roles in Resistance to Infection. *Journal of Experimental Medicine*, **194**, 181-187. https://doi.org/10.1084/jem.194.2.181

[36] Taylor, G.A., *et al.* (2000) Pathogen-Specific Loss of Host Resistance in Mice Lacking the IFN-γ-Inducible Gene IGTP. *Proceedings of the National Academy of Sciences of the United States of America*, **97**, 751-755. https://doi.org/10.1073/pnas.97.2.751

[37] Wang, Z.C., *et al.* (2008) Regulation of Innate Immune Responses by DAI (DLM-1/ZBP1) and Other DNA-Sensing Molecules. *Proceedings of the National Academy of Sciences of the United States of America*, **105**, 5477. https://doi.org/10.1073/pnas.0801295105

[38] Chuang, H.Y., Lee, E., Liu, Y.T., Lee, D. and Ideker, T. (2007) Network-Based Classification of Breast Cancer Metastasis. *Molecular Systems Biology*, **3**, 140. https://doi.org/10.1038/msb4100180

[39] Ideker, T., Ozier, O., Schwikowski, B. and Siegel, A.F. (2002) Discovering Regulatory and Signalling Circuits in Molecular Interaction Networks. *Bioinformatics*, **18**, 233-240. https://doi.org/10.1093/bioinformatics/18.suppl_1.S233

[40] He, X. and Zhang, J. (2006) Why Do Hubs Tend to Be Essential in Protein Net-

works? *PLOS Genetics*, **2**, e88. https://doi.org/10.1371/journal.pgen.0020088

[41] Jeong, H., Mason, S.P., Barabási, A.L. and Oltvai, Z.N. (2001) Lethality and Centrality in Protein Networks. *Nature*, **411**, 41-42. https://doi.org/10.1038/35075138

[42] Albert, R., Jeong, H. and Barabási, A.L. (2000) Error and Attack Tolerance of Complex Networks. *Nature*, **406**, 378-382. https://doi.org/10.1038/35019019

[43] Han, J.D.J., *et al.* (2004) Evidence for Dynamically Organized Modularity in the Yeast Protein-Protein Interaction Network. *Nature*, **430**, 88-93. https://doi.org/10.1038/nature02555

[44] Lee, D.S., Park, J., Kay, K.A., Christakis, N.A., Oltvai, Z.N. and Barabási, A.L. (2008) The Implications of Human Metabolic Network Topology for Disease Comorbidity. *Proceedings of the National Academy of Sciences of the United States of America*, **105**, 9880-9885. https://doi.org/10.1073/pnas.0802208105

Supplementary

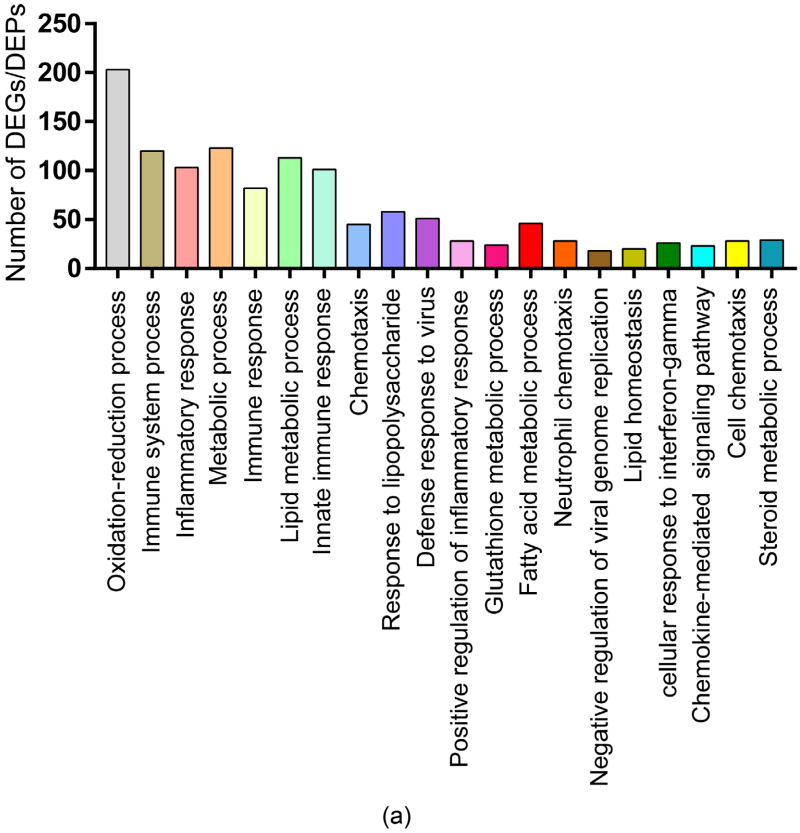

Figure S1. (a): Gene ontology for biological processes annotation of 2599 unique differentially expressed transcripts (DETs), (b): Gene ontology for biological processes annotation of 142 unique differentially expressed proteins (DEPs).

Table S1. List of 159 common differentially expressed genes/proteins.

Symbol	Description	Log_2 ratio at mRNA level	Log_2 ratio at protein level
Gm12250	Interferon-gamma-inducible p47 GTPase	5.2422	2.52406
S100a9	Calcium-binding regulatory protein of the S-100 family	6.58627	2.24458
Cd14	Leucine-rich repeat (LRR) protein	7.69689	2.1177
Igtp	Interferon gamma induced GTPase	3.20934	2.08236
Hpx	Hemopexin	3.40922	2.07279
Fga	Fibrinogen alpha chain	2.1146	2.07005
Fga	Fibrinogen alpha chain	3.05053	2.07005
H2-Aa	Histocompatibility 2, class II antigen A, alpha	3.345	2.0552
Fgb	Fibrinogen beta chain	2.86568	1.95568
Iigp1	Interferon inducible GTPase 1	3.60687	1.86592
Serpina3h	Serine (or cysteine) peptidase inhibitor, clade A, member 3H	4.68257	1.86592
Iigp1	Interferon inducible GTPase 1	8.21509	1.86592
Cd74	CD74 antigen (invariant polypeptide of major histocompatibility complex, class II antigen-associated)	3.8439	1.84157
Cd74	CD74 antigen (invariant polypeptide of major histocompatibility complex, class II antigen-associated)	3.85715	1.84157
Fgg	Fibrinogen gamma chain	2.87791	1.81967
Serpina3g	Serine (or cysteine) peptidase inhibitor, clade A, member 3G	6.33941	1.7476
Lcn2	Lipocalin 2	8.63454	1.73422
Lrg1	Leucine-rich HEV glycoprotein	4.27619	1.72814
Irgm1	Immunity-related GTPase family M protein 1	2.67923	1.7277
Arhgdib	Rho, GDP dissociation inhibitor (GDI) beta	2.99967	1.70487
H2-K1	Histocompatibility 2, K1, K region	1.14535	1.70443
Gbp2b	Guanylate binding protein 1	4.73796	1.67942
Itih4	Inter alpha-trypsin inhibitor, heavy chain 4	2.38453	1.67897
Itih4	Inter alpha-trypsin inhibitor, heavy chain 4	2.39753	1.67897
Anxa1	Annexin A1	2.50225	1.55631
Cp	Ceruloplasmin	2.90501	1.55483
Zbp1	Z-DNA-binding protein 1	3.81553	1.50894
Zbp1	Z-DNA-binding protein 1	4.7951	1.50894
Serpina3n	Serine protease inhibitor A3N	3.62354	1.49262
Fam49b	Protein FAM49B	2.25686	1.48491
Serping1	Plasma protease C1 inhibitor	1.275	1.46937
Tap1	Antigen peptide transporter 1	3.14638	1.45786
Egfr	Epidermal growth factor receptor	2.75854	1.45575
Egfr	Epidermal growth factor receptor	2.86143	1.45575

Continued

Itgb2	Integrin beta-2	3.53275	1.3989
Gbp6	Guanylate binding protein 6	3.70259	1.39726
Ifi44	Interferon-induced protein 44	3.04406	1.37518
Lgmn	Legumain	2.51305	1.37462
Ptpn1	Tyrosine-protein phosphatase non-receptor type 1	1.72369	1.36737
Samhd1	Deoxynucleoside triphosphate triphosphohydrolase SAMHD1	3.1593	1.35106
Samhd1	Deoxynucleoside triphosphate triphosphohydrolase SAMHD1	4.30208	1.35106
Tap2	Antigen peptide transporter 2	1.68331	1.33457
Tgm2	Protein-glutamine gamma-glutamyltransferase 2	2.065	1.32423
Hk3	Hexokinase-3	8.32981	1.301
Gbp2	Guanylate-binding protein 2	4.08145	1.26243
Orm1	Alpha-1-acid glycoprotein	4.17885	1.18142
Mvp	Major vault protein	1.63176	1.1375
Psmb9	Proteasome subunit beta	1.93217	1.13488
Lgals3bp	Galectin-3-binding protein	1.82358	1.11703
Iqgap1	Iqgap1 protein	2.33781	1.11703
G6pdx	Glucose-6-phosphate 1-dehydrogenase X	2.64194	1.06212
Fn1	Fibronectin	1.30989	1.05936
Lcp1	Plastin-2	3.09339	1.0552
Uba7	Ubiquitin-like modifier-activating enzyme 7	2.14919	1.03562
Xdh	Xanthine dehydrogenase	1.98023	1.03492
Vim	Vimentin	3.10772	1.02148
Fkbp5	Peptidyl-prolyl cis-trans isomerase FKBP5	2.24193	1.00288
Ifit1	Interferon-induced protein with tetratricopeptide	1.99492	0.996389
Clic1	Chloride intracellular channel protein 1	1.7613	0.950842
Siglec1	Sialic acid binding Ig-like lectin 1	3.01283	0.950842
Eppk1	Epiplakin	3.21857	0.944858
Cmpk2	UMP-CMP kinase 2, mitochondrial precursor	1.59206	0.938098
Anxa3	Annexin A3	1.96052	0.932817
Psmb8	Proteasome subunit beta type-8	1.889	0.92372
Cfh	Complement factor H	2.11825	0.877352
C3	Complement C3	1.46798	0.868687
Gatm	Glycine amidinotransferase, mitochondrial	1.53664	0.864731
Arpc1b	Actin-related protein 2/3 complex subunit 1B	1.59543	0.83754
Fth1	Ferritin heavy chain	2.28842	0.835924
Stat3	Signal transducer and activator of transcription 3	1.47583	0.835116
Stat3	Signal transducer and activator of transcription 3	1.92825	0.835116

Continued

Pml	Protein PML	2.04284	0.825379
Pld4	Phospholipase D4	2.4984	0.820485
Pzp	Alpha-2-macroglobulin	1.40793	0.727703
Fgl1	Fibrinogen-like protein 1	2.92407	0.712816
Ifit3	Interferon-induced protein with tetratricopeptide	1.57508	0.704872
Gbp4	Guanylate-binding protein 4	5.58761	0.644318
Gbp4	Guanylate-binding protein 4	6.78899	0.644318
Hmox1	Heme oxygenase 1	2.55661	0.641546
Tpm3	Tropomyosin alpha-3 chain	2.6855	0.641546
Pgm2	Phosphoglucomutase-2	−1.28895	0.636915
Oas1g	2'-5'-oligoadenylate synthase 1A	3.73967	0.627607
Dpp9	Dipeptidyl peptidase 9	1.17385	0.625738
Aldoa	Fructose-bisphosphate aldolase A	2.43601	0.602172
Rab7	Ras-related protein Rab-7a	1.22934	0.593593
Serpina3k	Serine protease inhibitor A3K	1.24149	0.591679
Eif1a	Eukaryotic translation initiation factor 1A	2.00872	0.591679
Apoc3	Apolipoprotein C-III	−1.86959	−0.58857
Ndufb5	NADH dehydrogenase (Ubiquinone) 1 beta	−1.5095	−0.59292
Inmt	Indolethylamine N-methyltransferase	−9.1501	−0.59728
Aadac	Arylacetamide deacetylase	−2.27363	−0.59728
Ces2a	Pyrethroid hydrolase Ces2a	−4.30604	−0.60384
Gstm1	Glutathione S-transferase Mu 1	−4.00942	−0.60384
Abcb11	Bile salt export pump	−3.11676	−0.60604
Gcsh	Glycine cleavage system H protein	−2.04067	−0.60604
Aacs	Acetoacetyl-CoA synthetase	−2.32445	−0.60823
Echdc1	Isoform 2 of Ethylmalonyl-CoA decarboxylase	−1.83671	−0.61043
Hacl1	2-hydroxyacyl-CoA lyase 1	−1.56776	−0.61485
Slc2a2	Solute carrier family 2, facilitated glucose	−3.56513	−0.62816
Pklr	Pyruvate kinase	−2.32813	−0.63039
Ugp2	Ugp2 protein	−2.41366	−0.63263
Ndufb6	NADH dehydrogenase [ubiquinone] 1 beta subcomplex subunit 6	−1.3219	−0.63487
Fkbp8	FK-506-binding protein 38	−1.36783	−0.63711
Tymp	Thymidine phosphorylase	−2.93575	−0.64611
Abat	4-aminobutyrate aminotransferase	−2.45914	−0.70369
Abca8a	ABC transporter A subfamily member, A8a	−4.36047	−0.82113
Abcd3	Putative uncharacterized protein	−1.8338	−0.78588
Acaa1b	Putative uncharacterized protein	−7.88352	−1.59946

Continued

Acadsb	Acyl-Coenzyme A dehydrogenase, short/branched chain	−1.70773	−0.67346
Acsl1	Long-chain-fatty-acid-CoA ligase 1	−2.39423	−0.78588
Acss3	Acyl-CoA synthetase short-chain family member 3	−2.4508	−0.74662
Adck3	Chaperone activity of bc1 complex-like	−5.68017	−0.87832
Afmid	Kynurenine formamidase	−4.21945	−0.84166
Agxt	Isoform Peroxisomal of Serine-pyruvate aminotransferase	−3.10264	−0.64837
Aldh3a2	Aldehyde dehydrogenase	−3.54492	−0.6529
Apoa2	Apolipoprotein A-II	−2.94256	−1.02327
Atp5j	ATP synthase-coupling factor 6	−1.0603	−0.81097
Bbox1	Gamma-butyrobetaine dioxygenase	−2.83706	−0.96578
Cat	Catalase	−3.75739	−0.78837
Ces1c	Carboxylesterase 1C	−4.18488	−1.39973
Ces1e	Carboxylesterase 1E	−7.19784	−1.33643
Cyp1a2	Cytochrome P450 family 1 subfamily a polypeptide 2	−6.90204	−1.30401
Cyp2a22	Cyp2a22 protein	−5.84631	−1.38836
Cyp2b9	Cytochrome P450 2B9	−6.8513	−1.13289
Cyp2c29	Cytochrome P450 2C29	−7.58211	−1.47794
Cyp2c50	Isoform 2 of Cytochrome P450 2C50	−9.30694	−0.99712
Cyp2c50	Isoform 2 of Cytochrome P450 2C50	−8.29929	−0.99712
Cyp2c50	Isoform 2 of Cytochrome P450 2C50	−8.23267	−0.99712
Cyp2c54	Cytochrome P450 2C54	−9.23214	−0.78339
Cyp3a11	Cytochrome P450 3A11	−3.8865	−0.9105
Cyp3a16	Cytochrome P450, family 3, subfamily a, polypeptide 16	−3.50156	−0.82368
Cyp3a25	Cytochrome P450 3A25	−3.91863	−1.27579
Cyp4a10	Cytochrome P450 4A10	−4.88865	−1.152
Cyp8b1	7-alpha-hydroxycholest-4-en-3-one 12-alpha-hydroxylase	−4.80208	−0.92413
Ehhadh	Peroxisomal bifunctional enzyme	−3.15994	−1.08009
Etnppl	Ethanolamine-phosphate phospho-lyase	−5.33103	−1.18771
Fads2	Delta-6 desaturase (Fragment)	−3.0613	−0.83908
Fmo3	Dimethylaniline monooxygenase [N-oxide-forming] 3	−5.56319	−1.08927
Gck	Isoform 2 of Glucokinase	−4.13301	−0.75633
Gls2	Glutaminase liver isoform	−2.78405	−0.75147
Gm4952	Glycine N-acyltransferase-like protein	−5.85372	−0.76366
Hao2	Putative uncharacterized protein	−13.3741	−1.50226
Hsd17b6	17-beta-hydroxysteroid dehydrogenase type 6	−2.14597	−0.68038
Hsd3b3	3 beta-hydroxysteroid dehydrogenase/Delta 5->4-isomerase type 3	−9.32331	−0.94342
Hsd3b3	3 beta-hydroxysteroid dehydrogenase/Delta 5->4-isomerase type 3	−8.79514	−0.94342

Continued

Ido2	Indoleamine 2,3-dioxygenase 2	−1.98034	−0.73217
Lactb2	Beta-lactamase-like protein 2	−2.51727	−1.04394
Me1	NADP-dependent malic enzyme	−2.04421	−0.72738
Oat	Putative uncharacterized protein	−2.13265	−0.83393
Pah	Putative uncharacterized protein	−2.67804	−1.55216
Pygl	Glycogen phosphorylase, liver form	−2.27605	−0.73697
Reep6	Receptor expression-enhancing protein 6	−2.1388	−0.78588
Reep6	Receptor expression-enhancing protein 6	−1.81864	−0.78588
Sult2a1	Bile salt sulfotransferase 1	−2.52348	−1.54372
Sult2a5	Sulfotransferase family 2A member 1 family	−3.87193	−1.28279
Thrsp	Thyroid hormone-inducible hepatic protein	−5.47987	−1.18442
Ttc36	Tetratricopeptide repeat protein 36	−2.27664	−1.43051
Ttr	Transthyretin	−2.80447	−0.78339
Uqcrfs1	Cytochrome b-c1 complex subunit Rieske	−1.23339	−0.76857

Table S2. List of 86 common up-regulated genes/proteins.

Symbol	Description	Log_2 ratio at mRNA level	Log_2 ratio at protein level
Cd74	CD74 antigen (invariant polypeptide of major histocompatibility complex, class II antigen-associated)	3.843901	1.841571
Cd74	CD74 antigen (invariant polypeptide of major histocompatibility complex, class II antigen-associated)	3.857146	1.841571
Egfr	Epidermal growth factor receptor	2.86143	1.455755
Egfr	Epidermal growth factor receptor	2.758544	1.455755
Fga	Fibrinogen alpha chain	3.050532	2.070046
Fga	Fibrinogen alpha chain	2.114599	2.070046
Gbp4	Guanylate-binding protein 4	6.788995	0.644318
Gbp4	Guanylate-binding protein 4	5.587608	0.644318
Iigp1	Interferon inducible GTPase 1	8.21509	1.865919
Iigp1	Interferon inducible GTPase 1	3.606874	1.865919
Itih4	Inter alpha-trypsin inhibitor, heavy chain 4	2.384532	1.678973
Itih4	Inter alpha-trypsin inhibitor, heavy chain 4	2.397529	1.678973
Samhd1	Deoxynucleoside triphosphate triphosphohydrolase SAMHD1	3.159299	1.351063
Samhd1	Deoxynucleoside triphosphate triphosphohydrolase SAMHD1	4.302077	1.351063
Stat3	Signal transducer and activator of transcription 3	1.928252	0.835116
Stat3	Signal transducer and activator of transcription 3	1.475831	0.835116
Zbp1	Z-DNA-binding protein 1	4.795101	1.508936

Continued

Zbp1	Z-DNA-binding protein 1	3.815526	1.508936
Aldoa	Fructose-bisphosphate aldolase A	2.436009	0.602172
Anxa1	Annexin A1	2.502246	1.556307
Anxa3	Annexin A3	1.960524	0.932817
Arhgdib	Rho, GDP dissociation inhibitor (GDI) beta	2.99967	1.704872
Arpc1b	Actin-related protein 2/3 complex subunit 1B	1.595427	0.83754
C3	Complement C3	1.467976	0.868687
Cd14	Leucine-rich repeat (LRR) protein	7.69689	2.117695
Cfh	Complement factor H	2.118245	0.877352
Clic1	Chloride intracellular channel protein 1	1.761302	0.950842
Cmpk2	UMP-CMP kinase 2, mitochondrial precursor	1.592055	0.938098
Cp	Ceruloplasmin	2.905007	1.554834
Dpp9	Dipeptidyl peptidase 9	1.173849	0.625738
Eif1a	Eukaryotic translation initiation factor 1A	2.008719	0.591679
Eppk1	Epiplakin	3.218575	0.944858
Fam49b	Protein FAM49B	2.256859	1.484911
Fgb	Fibrinogen beta chain	2.865676	1.955685
Fgg	Fibrinogen gamma chain	2.877913	1.819668
Fgl1	Fibrinogen-like protein 1	2.924074	0.712816
Fkbp5	Peptidyl-prolyl cis-trans isomerase FKBP5	2.241925	1.002882
Fn1	Fibronectin	1.309886	1.059355
Fth1	Ferritin heavy chain	2.288422	0.835924
G6pdx	Glucose-6-phosphate 1-dehydrogenase X	2.641936	1.062122
Gatm	Glycine amidinotransferase, mitochondrial	1.536639	0.864731
Gbp2	Guanylate-binding protein 2	4.081453	1.262433
Gbp2b	Guanylate binding protein 1	4.737961	1.679424
Gbp6	Guanylate binding protein 6	3.702585	1.397255
Gm12250	Interferon-gamma-inducible p47 GTPase	5.242204	2.524064
H2-Aa	Histocompatibility 2, class II antigen A, alpha	3.345002	2.055196
H2-K1	Histocompatibility 2, K1, K region	1.145345	1.704429
Hk3	Hexokinase-3	8.329807	1.301002
Hmox1	Heme oxygenase 1	2.556608	0.641546
Hpx	Hemopexin	3.409221	2.072792
Ifi44	Interferon-induced protein 44	3.044058	1.375178
Ifit1	Interferon-induced protein with tetratricopeptide	1.994923	0.996389

Continued

Ifit3	Interferon-induced protein with tetratricopeptide	1.575076	0.704872
Igtp	Interferon gamma induced GTPase	3.20934	2.082362
Iqgap1	Iqgap1 protein	2.33781	1.11703
Irgm1	Immunity-related GTPase family M protein 1	2.67923	1.727703
Itgb2	Integrin beta-2	3.532746	1.398898
Lcn2	Lipocalin 2	8.63454	1.734222
Lcp1	Plastin-2	3.093387	1.055196
Lgals3bp	Galectin-3-binding protein	1.823581	1.11703
Lgmn	Legumain	2.513047	1.374622
Lrg1	Leucine-rich HEV glycoprotein	4.276191	1.728138
Mvp	Major vault protein	1.63176	1.137504
Oas1g	2'-5'-oligoadenylate synthase 1A	3.739666	0.627607
Orm1	Alpha-1-acid glycoprotein	4.178853	1.181421
Pld4	Phospholipase D4	2.498401	0.820485
Pml	Protein PML	2.042842	0.825379
Psmb8	Proteasome subunit beta type-8	1.889003	0.92372
Psmb9	Proteasome subunit beta type-9	1.932167	1.134878
Ptpn1	Tyrosine-protein phosphatase non-receptor type 1	1.72369	1.367371
Pzp	Alpha-2-macroglobulin	1.407928	0.727703
Rab7	Ras-related protein Rab-7a	1.229339	0.593593
S100a9	Calcium-binding regulatory protein of the S-100 family	6.586273	2.244583
Serpina3g	Serine (or cysteine) peptidase inhibitor, clade A, member 3G	6.33941	1.747602
Serpina3h	Serine (or cysteine) peptidase inhibitor, clade A, member 3H	4.682567	1.865919
Serpina3k	Serine protease inhibitor A3K	1.241492	0.591679
Serpina3n	Serine protease inhibitor A3N	3.623544	1.492622
Serping1	Plasma protease C1 inhibitor	1.275004	1.469365
Siglec1	Sialic acid binding Ig-like lectin 1	3.012835	0.950842
Tap1	Antigen peptide transporter 1	3.146375	1.457857
Tap2	Antigen peptide transporter 2	1.683309	1.334568
Tgm2	Protein-glutamine gamma-glutamyltransferase 2	2.065	1.324235
Tpm3	Tropomyosin alpha-3 chain	2.685497	0.641546
Uba7	Ubiquitin-like modifier-activating enzyme 7	2.149189	1.035624
Vim	Vimentin	3.107717	1.02148
Xdh	Xanthine dehydrogenase	1.980225	1.03492

Table S3. List of common 72 down-regulated genes/proteins.

Symbol	Description	Log_2 ratio at mRNA level	Log_2 ratio at protein level
Cyp2c50	Isoform 2 of Cytochrome P450 2C50	−9.30694	−0.99712
Cyp2c50	Isoform 2 of Cytochrome P450 2C50	−8.23267	−0.99712
Cyp2c50	Isoform 2 of Cytochrome P450 2C50	−8.29929	−0.99712
Hsd3b3	3 beta-hydroxysteroid dehydrogenase/Delta 5->4-isomerase type 3	−9.32331	−0.94342
Hsd3b3	3 beta-hydroxysteroid dehydrogenase/Delta 5->4-isomerase type 3	−8.79514	−0.94342
Reep6	Receptor expression-enhancing protein 6	−1.81864	−0.78588
Reep6	Receptor expression-enhancing protein 6	−2.1388	−0.78588
Aacs	Acetoacetyl-CoA synthetase	−2.32445	−0.60823
Aadac	Arylacetamide deacetylase	−2.27363	−0.59728
Abat	4-aminobutyrate aminotransferase	−2.45914	−0.70369
Abca8a	ABC transporter A subfamily member, A8a	−4.36047	−0.82113
Abcb11	Bile salt export pump	−3.11676	−0.60603
Abcd3	Putative uncharacterized protein	−1.8338	−0.78588
Acaa1b	Putative uncharacterized protein	−7.88352	−1.59946
Acadsb	Acyl-Coenzyme A dehydrogenase, short/branched chain	−1.70773	−0.67346
Acsl1	Long-chain-fatty-acid-CoA ligase 1	−2.39423	−0.78588
Acss3	Acyl-CoA synthetase short-chain family member 3	−2.4508	−0.74662
Adck3	Chaperone activity of bc1 complex-like	−5.68017	−0.87832
Afmid	Kynurenine formamidase	−4.21945	−0.84166
Agxt	Isoform Peroxisomal of Serine-pyruvate aminotransferase	−3.10264	−0.64837
Aldh3a2	Aldehyde dehydrogenase	−3.54492	−0.6529
Apoa2	Apolipoprotein A-II	−2.94256	−1.02327
Apoc3	Apolipoprotein C-III	−1.86959	−0.58857
Atp5j	ATP synthase-coupling factor 6	−1.0603	−0.81097
Bbox1	Gamma-butyrobetaine dioxygenase	−2.83706	−0.96578
Cat	Catalase	−3.75739	−0.78836
Ces1c	Carboxylesterase 1C	−4.18488	−1.39973
Ces1e	Carboxylesterase 1E	−7.19784	−1.33643
Ces2a	Pyrethroid hydrolase Ces2a	−4.30604	−0.60384
Cyp1a2	Cytochrome P450 family 1 subfamily a polypeptide 2	−6.90204	−1.30401
Cyp2a22	Cyp2a22 protein	−5.84631	−1.38836
Cyp2b9	Cytochrome P450 2B9	−6.8513	−1.13289
Cyp2c29	Cytochrome P450 2C29	−7.58211	−1.47794
Cyp2c54	Cytochrome P450 2C54	−9.23214	−0.78339
Cyp3a11	Cytochrome P450 3A11	−3.8865	−0.9105

Continued

Cyp3a16	Cytochrome P450, family 3, subfamily a, polypeptide 16	−3.50156	−0.82368
Cyp3a25	Cytochrome P450 3A25	−3.91863	−1.27579
Cyp4a10	Cytochrome P450 4A10	−4.88865	−1.152
Cyp8b1	7-alpha-hydroxycholest-4-en-3-one 12-alpha-hydroxylase	−4.80208	−0.92413
Echdc1	Isoform 2 of Ethylmalonyl-CoA decarboxylase	−1.83671	−0.61043
Ehhadh	Peroxisomal bifunctional enzyme	−3.15994	−1.08009
Etnppl	Ethanolamine-phosphate phospho-lyase	−5.33103	−1.18771
Fads2	Delta-6 desaturase (Fragment)	−3.0613	−0.83908
Fkbp8	FK-506-binding protein 38	−1.36783	−0.63711
Fmo3	Dimethylaniline monooxygenase [N-oxide-forming] 3	−5.56319	−1.08927
Gck	Isoform 2 of Glucokinase	−4.13301	−0.75633
Gcsh	Glycine cleavage system H protein	−2.04067	−0.60603
Gls2	Glutaminase liver isoform	−2.78405	−0.75147
Gm4952	Glycine N-acyltransferase-like protein	−5.85372	−0.76366
Gstm1	Glutathione S-transferase Mu 1	−4.00942	−0.60384
Hacl1	2-hydroxyacyl-CoA lyase 1	−1.56776	−0.61485
Hao2	Putative uncharacterized protein	−13.3741	−1.50226
Hsd17b6	17-beta-hydroxysteroid dehydrogenase type 6	−2.14597	−0.68038
Ido2	Indoleamine 2,3-dioxygenase 2	−1.98034	−0.73216
Inmt	Indolethylamine N-methyltransferase	−9.1501	−0.59728
Lactb2	Beta-lactamase-like protein 2	−2.51727	−1.04394
Me1	NADP-dependent malic enzyme	−2.04421	−0.72738
Ndufb5	NADH dehydrogenase (Ubiquinone) 1 beta	−1.5095	−0.59292
Ndufb6	NADH dehydrogenase [ubiquinone] 1 beta subcomplex subunit 6	−1.3219	−0.63487
Oat	Putative uncharacterized protein	−2.13265	−0.83393
Pah	Putative uncharacterized protein	−2.67804	−1.55216
Pklr	Pyruvate kinase	−2.32813	−0.63039
Pygl	Glycogen phosphorylase, liver form	−2.27605	−0.73697
Slc2a2	Solute carrier family 2, facilitated glucose	−3.56513	−0.62816
Sult2a1	Bile salt sulfotransferase 1	−2.52348	−1.54372
Sult2a5	Sulfotransferase family 2A member 1 family	−3.87193	−1.28279
Thrsp	Thyroid hormone-inducible hepatic protein	−5.47987	−1.18442
Ttc36	Tetratricopeptide repeat protein 36	−2.27664	−1.43051
Ttr	Transthyretin	−2.80447	−0.78339
Tymp	Thymidine phosphorylase	−2.93575	−0.64611
Ugp2	Ugp2 protein	−2.41366	−0.63263
Uqcrfs1	Cytochrome b-c1 complex subunit Rieske	−1.23339	−0.76857

Table S4. List of up-regulated genes/proteins and associated GO terms.

Term	Description	Genes	FDR
		Biological processes	
GO:0002376	Immune system process	H2-K1, IRGM1, C3, S100A9, PML, ANXA1, SAMHD1, SERPING1, GBP2B, PSMB8, CD74, PSMB9, LCN2, IFIT3, FGG, IFIT1, FGA, SERPINA3G, FGB, TAP2, TAP1, CFH, H2-AA, IIGP1, CD14, ZBP1	5.75E−21
GO:0045087	Innate immune response	IRGM1, C3, S100A9, ANXA1, PML, SAMHD1, SERPING1, IFIT3, LCN2, FGG, IFIT1, FGA, FGB, CFH, IIGP1, CD14, ZBP1	4.88E−09
GO:0035458	Cellular response to interferon-beta	IFIT3, IFIT1, IRGM1, GBP6, IGTP, IIGP1, GBP2B, GBP2	3.57E−07
GO:0002250	Adaptive immune response	FGG, FGA, FGB, SERPINA3G, TAP2, TAP1, ANXA1, CD74	0.001988979
GO:0006953	Acute-phase response	ORM1, SERPINA3N, ITIH4, STAT3, FN1	0.016555934
GO:0034097	Response to cytokine	SERPINA3K, SERPINA3N, SERPINA3G, ITIH4, PML, STAT3	0.026453654
GO:0006879	Cellular iron ion homeostasis	LCN2, HPX, HMOX1, CP, FTH1	0.045710521
GO:0051607	Defense response to virus	IFIT3, IFIT1, PML, SAMHD1, GBP2B, OAS1G, ZBP1	0.080418113
GO:0019882	~antigen processing and presentation	H2-K1, H2-AA, CD74, PSMB8, PSMB9	0.094415132
GO:0010466	Negative regulation of peptidase activity	SERPINA3K, SERPINA3N, PZP, SERPINA3G, ITIH4, SERPING1	0.154739303
GO:0043434	Response to peptide hormone	SERPINA3K, SERPINA3N, GATM, SERPINA3G, ANXA1	0.306643017
GO:0007160	Cell-matrix adhesion	FGG, FGA, FGB, ITGB2, FN1	0.395726443
GO:0007596	Blood coagulation	FGG, FGA, C3, FGB, SERPING1	0.52544175
GO:0070374	Positive regulation of ERK1 and ERK2 cascade	EGFR, FGG, FGA, C3, FGB, CD74	1.369527162
GO:0045766	Positive regulation of angiogenesis	C3, LRG1, HMOX1, ITGB2, ANXA3	2.056385341
GO:0071222	Cellular response to lipopolysaccharide	LCN2, GBP6, GBP2, CD14, CMPK2	13.58949423
GO:0006955	Immune response	H2-K1, H2-AA, OAS1G, FTH1, CD74	29.72515146
		Cellular component	

Continued

GO:0070062	Extracellular exosome	ALDOA, FKBP5, C3, LGMN, VIM, G6PDX, S100A9, ITGB2, FTH1, IQGAP1, CD74, RAB7, TPM3, FGG, LGALS3BP, FAM49B, FGA, LRG1, FGB, ITIH4, CFH, TGM2, FGL1, FN1, ARHGDIB, H2-K1, GBP6, GATM, ANXA1, SERPING1, CLIC1, PSMB8, ANXA3, PSMB9, LCN2, ARPC1B, SERPINA3K, SERPINA3N, HPX, CP, GBP4, LCP1, CD14, MVP	7.76E−16
GO:0072562	Blood microparticle	C3, SERPING1, CLIC1, SERPINA3K, SERPINA3N, LGALS3BP, FGG, FGA, HPX, FGB, ITIH4, CFH, CP, FN1	3.79E−12
GO:0005615	Extracellular space	XDH, ALDOA, PZP, C3, S100A9, LGALS3BP, FGG, FGA, LRG1, FGB, CFH, FN1, ANXA1, SERPING1, CLIC1, LCN2, SERPINA3K, ORM1, SERPINA3N, SERPINA3H, HPX, SERPINA3G, CP, LCP1, CD14	9.32E−07
GO:0005576	Extracellular region	XDH, PZP, C3, S100A9, ANXA1, SERPING1, GBP2B, FTH1, LCN2, ORM1, SERPINA3K, SIGLEC1, FGG, SERPINA3N, LGALS3BP, FGA, HPX, FGB, ITIH4, CFH, CP, FGL1, CD14, FN1	9.38E−05
GO:0005829	Cytosol	XDH, G6PDX, VIM, ANXA1, UBA7, PML, PSMB8, STAT3, RAB7, CMPK2, PSMB9, LCN2, IGTP, HMOX1, HK3, TGM2, DPP9, PTPN1, LCP1, ZBP1, ARHGDIB	0.009533
GO:0030670	Phagocytic vesicle membrane	H2-K1, IRGM1, TAP1, ANXA3, RAB7	0.037403
GO:0009897	External side of plasma membrane	H2-K1, FGG, FGA, FGB, H2-AA, CD74, CD14	1.601494
GO:0009986	Cell surface	EGFR, H2-K1, FGG, FGA, FGB, ANXA1, ITGB2, CD74, CD14	3.221346
GO:0005737	Cytoplasm	XDH, ALDOA, FKBP5, VIM, G6PDX, S100A9, PML, GBP2B, IQGAP1, RAB7, TPM3, FGG, FGA, FGB, ITIH4, TGM2, CFH, IIGP1, DPP9, ARHGDIB, ZBP1, EGFR, EPPK1, ANXA1, IFI44, CLIC1, PSMB8, ANXA3, STAT3, PSMB9, IFIT3, ARPC1B, IFIT1, SERPINA3G, PTPN1, GBP2, LCP1, MVP	4.382999
GO:0005925	Focal adhesion	EGFR, ARPC1B, VIM, ANXA1, TGM2, IQGAP1, LCP1	4.50095
GO:0005913	Cell-cell adherens junction	EGFR, ALDOA, ANXA1, PTPN1, CLIC1, IQGAP1	8.377285
GO:0005783	Endoplasmic reticulum	EGFR, H2-K1, IRGM1, TAP2, HMOX1, TAP1, PLD4, PML, TGM2, IIGP1, PTPN1, CD74	12.93212

Continued

GO:0016020	Membrane	ALDOA, FKBP5, G6PDX, S100A9, PML, ITGB2, GBP2B, IQGAP1, CD74, RAB7, LGALS3BP, FAM49B, IGTP, TAP2, HMOX1, TAP1, TGM2, IIGP1, ARHGDIB, EGFR, H2-K1, IRGM1, GBP6, GATM, PLD4, ANXA1, CLIC1, ANXA3, SIGLEC1, GM12250, H2-AA, PTPN1, GBP4, GBP2, CD14, LCP1, MVP	19.81221
GO:0031012	Extracellular matrix	LGALS3BP, VIM, S100A9, TGM2, FN1	27.42094
GO:0031410	Cytoplasmic vesicle	IRGM1, GBP6, ANXA1, PTPN1, GBP2B, GBP2, RAB7	36.50644
GO:0005764	Lysosome	IRGM1, LGMN, H2-AA, CD74, RAB7	37.37253
		Molecular function	
GO:0003924	GTPase activity	IRGM1, GBP6, IGTP, IIGP1, GBP2B, GBP4, GBP2, RAB7, ARHGDIB	0.002934
GO:0005525	GTP binding	IRGM1, GBP6, IGTP, GM12250, TGM2, IIGP1, GBP2B, GBP4, GBP2, RAB7	0.034515
GO:0004867	Serine-type endopeptidase inhibitor activity	SERPINA3K, SERPINA3N, PZP, SERPINA3G, ITIH4, SERPING1	0.196148
GO:0030414	Peptidase inhibitor activity	SERPINA3K, SERPINA3N, PZP, SERPINA3G, ITIH4, SERPING1	0.196148
GO:0042802	Identical protein binding	EGFR, IFIT3, VIM, G6PDX, IIGP1, DPP9, LCP1, STAT3, FN1	5.139194
GO:0098641	Cadherin binding involved in cell-cell adhesion	EGFR, ALDOA, ANXA1, PTPN1, CLIC1, IQGAP1	7.269523
GO:0019901	Protein kinase binding	EGFR, VIM, ITGB2, PTPN1, IQGAP1, STAT3, MVP	10.86314
GO:0005198	Structural molecule activity	FGG, FGA, FGB, VIM, ANXA1	19.00636
GO:0042803	Protein homodimerization activity	LCN2, XDH, FGG, TAP2, HMOX1, TAP1, G6PDX, ANXA1, PML	19.36988
GO:0005515	Protein binding	XDH, C3, VIM, PML, ITGB2, IQGAP1, CD74, RAB7, TPM3, LGALS3BP, FAM49B, TAP2, ITIH4, FN1, EGFR, PLD4, ANXA1, STAT3, IFIT3, LCN2, SERPINA3K, SIGLEC1, IFIT1, H2-AA, GBP4, LCP1	22.71878

Table S5. List of down-regulated genes/proteins and associated GO terms.

Term	Description	Genes	FDR
		Biological processes	
GO:0055114	Oxidation-reduction process	ME1, HSD3B3, ACADSB, NDUFB5, NDUFB6, CYP3A25, EHHADH, CYP2B9, PAH, UQCRFS1, ALDH3A2, BBOX1, FMO3, HSD17B6, CAT, CYP2C54, CYP3A16, CYP3A11, CYP2C29, IDO2, FADS2, CYP1A2, CYP2C50, CYP4A10, HAO2, CYP8B1	2.60E−17
GO:0008152	Metabolic process	HSD3B3, ACADSB, EHHADH, ECHDC1, PAH, ACSS3, ALDH3A2, AFMID, GSTM1, AADAC, TYMP, ACSL1, PYGL, PKLR, AACS, ACAA1B, UGP2	1.89E−09
GO:0006629	Lipid metabolic process	HACL1, ACADSB, ACSL1, SULT2A1, EHHADH, APOC3, HSD17B6, FADS2, CYP1A2, AACS, ACAA1B, THRSP	3.76E−04
GO:0006631	Fatty acid metabolic process	CYP4A10, ACADSB, APOA2, ACSL1, EHHADH, FADS2, AACS, ACAA1B	0.0011
GO:0019373	Epoxygenase P450 pathway	CYP2A22, CYP2C54, CYP2B9, CYP2C29, CYP2C50	0.003784
GO:0042493	Response to drug	APOA2, ACSL1, ABCB11, ABAT, ABCD3, CAT, UQCRFS1, AACS	0.169252
GO:0006810	Transport	TTR, NDUFB5, APOA2, NDUFB6, ABCB11, SLC2A2, APOC3, ABCA8A, ABCD3, FADS2, UQCRFS1, ATP5J	38.61568
		Cellular component	
GO:0031090	Organelle membrane	CYP4A10, AADAC, CYP2C54, CYP3A16, CYP3A25, CYP3A11, CYP2B9, FMO3, CYP2C29, CYP1A2, CYP8B1, CYP2C50	1.00E−11
GO:0005739	Mitochondrion	ME1, ETNPPL, HSD3B3, FKBP8, ACADSB, NDUFB5, NDUFB6, EHHADH, UQCRFS1, AGXT, ACSS3, ALDH3A2, BBOX1, GLS2, ACSL1, ABCD3, GCSH, CAT, ACAA1B, ATP5J, LACTB2, GM4952, GCK, HAO2, ABAT, OAT	4.24E−08
GO:0005789	Endoplasmic reticulum membrane	REEP6, HSD3B3, CYP2C54, CYP3A25, CYP3A16, CYP3A11, CYP2B9, CYP2C29, FADS2, CYP1A2, ALDH3A2, CYP2C50, AADAC, CYP4A10, ACSL1, FMO3, CYP8B1	6.94E−07
GO:0043231	Intracellular membrane-bounded organelle	CYP2C54, CYP3A25, CYP3A16, CYP3A11, CYP2B9, CYP2C29, CYP1A2, ALDH3A2, CYP2C50, AADAC, CYP4A10, ACSL1, FMO3, ABCD3, HSD17B6, CAT, CYP8B1	1.56E−06
GO:0005783	Endoplasmic reticulum	REEP6, HSD3B3, CYP2C54, CYP3A25, CYP3A16, CYP2B9, CYP3A11, CYP2C29, FADS2, CYP1A2, ALDH3A2, CYP2C50, AADAC, CYP4A10, ACSL1, FMO3, HSD17B6, CAT, CES1E, CYP8B1, CES1C	3.58E−06

Continued

GO:0005777	Peroxisome	HACL1, ACSL1, EHHADH, HAO2, ABCD3, CAT, ACAA1B, AGXT	2.27E−04
GO:0005829	Cytosol	ME1, SULT2A5, SULT2A1, EHHADH, ECHDC1, ALDH3A2, INMT, AFMID, TYMP, APOA2, GCK, SLC2A2, APOC3, PKLR, CAT, AACS, THRSP	0.145049
GO:0005743	Mitochondrial inner membrane	HSD3B3, NDUFB5, NDUFB6, ABCA8A, ABCD3, UQCRFS1, ALDH3A2, ATP5J	0.259456
GO:0005759	Mitochondrial matrix	GLS2, ACADSB, ABAT, OAT, AGXT, LACTB2	0.369843
GO:0070062	Extracellular exosome	ACADSB, ABCB11, ECHDC1, PAH, ALDH3A2, BBOX1, CYP4A10, TTR, APOA2, PYGL, APOC3, PKLR, HAO2, ABAT, CAT, UGP2	20.70699
		Molecular function	
GO:0016491	Oxidoreductase activity	ME1, HSD3B3, ACADSB, CYP2C54, CYP3A25, CYP3A16, CYP2B9, EHHADH, CYP3A11, CYP2C29, IDO2, FADS2, PAH, CYP1A2, UQCRFS1, ALDH3A2, BBOX1, CYP2C50, CYP4A10, HAO2, FMO3, HSD17B6, CAT, CYP8B1	5.09E−15
GO:0004497	Monooxygenase activity	CYP4A10, CYP2C54, CYP3A16, CYP3A25, CYP3A11, CYP2B9, FMO3, CYP2C29, PAH, CYP1A2, CYP8B1, CYP2C50	1.79E−10
GO:0020037	Heme binding	CYP3A25, CYP3A16, CYP2C54, CYP3A11, CYP2B9, CYP2C29, IDO2, CYP1A2, CYP2C50, CYP4A10, CYP2A22, CAT, CYP8B1	1.52E−09
GO:0005506	Iron ion binding	CYP3A25, CYP3A16, CYP2C54, CYP3A11, CYP2B9, CYP2C29, PAH, CYP1A2, BBOX1, CYP2C50, CYP4A10, CYP2A22, CYP8B1	1.47E−08
GO:0070330	Aromatase activity	CYP2C54, CYP3A16, CYP3A25, CYP3A11, CYP2B9, CYP2C29, CYP1A2, CYP2C50	5.45E−08
GO:0016705	Oxidoreductase activity, acting on paired donors, with incorporation or reduction of molecular oxygen	CYP4A10, CYP2C54, CYP3A16, CYP3A25, CYP3A11, CYP2B9, CYP2C29, CYP1A2, CYP8B1, CYP2C50	9.66E−08
GO:0003824	Catalytic activity	ETNPPL, HACL1, HSD3B3, EHHADH, ECHDC1, PAH, ACSS3, AGXT, ACSL1, PYGL, PKLR, HAO2, ABAT, AACS, OAT, ACAA1B	1.39E−07
GO:0016712	Oxidoreductase activity, acting on paired donors, with incorporation or reduction of molecular oxygen, reduced flavin or flavoprotein as one donor, and incorporation of one atom of oxygen	CYP2A22, CYP3A16, CYP3A25, CYP3A11, CYP2B9, CYP2C29, CYP1A2	1.03E−05

Continued

GO:0008392	Arachidonic acid epoxygenase activity	CYP4A10, CYP2A22, CYP2C54, CYP2B9, CYP2C29, CYP2C50	8.90E−04
GO:0008395	Steroid hydroxylase activity	CYP2A22, CYP2C54, CYP2B9, CYP2C29, CYP2C50	0.053216
GO:0030170	Pyridoxal phosphate binding	ETNPPL, PYGL, ABAT, OAT, AGXT	0.057234
GO:0016740	Transferase activity	SULT2A5, ETNPPL, SULT2A1, AGXT, INMT, GSTM1, GM4952, TYMP, GCK, PYGL, PKLR, ABAT, OAT, ACAA1B, UGP2	0.788706
GO:0042803	Protein homodimerization activity	GSTM1, APOA2, PYGL, ABAT, ABCD3, PAH, CAT, AGXT, THRSP	9.244787
GO:0046872	Metal ion binding	ME1, HACL1, CYP2C54, CYP3A25, CYP3A16, CYP3A11, CYP2B9, CYP2C29, IDO2, PAH, CYPF2, UQCRFS1, LACTB2, BBOX1, CYP2C50, CYP4A10, PKLR, ABAT, CAT, CYP8B1, UGP2	14.20634
GO:0042802	Identical protein binding	ETNPPL, TTR, HACL1, FKBP8, ABAT, OAT, UGP2	27.05591